To the Graduate Council:

I am submitting herewith a thesis written by Edwin A. McDougle, Jr. entitled "A Comparison of Experimental and Computed Lateral Load Distribution for Two Continuous Steel Girder Highway Bridges." I recommend that it be accepted in partial fulfillment of the requirements for the degree of Master of Science, with a major in Civil Engineering.

Edwin G. Burdette

Edwin G. Burdette
Major Professor

We have read this thesis
and recommend its acceptance

D. W. Goodpasture

Edwin P. Foster

Accepted for the Council

Hilton A. Smith

Vice Chancellor
Graduate Studies and Research

p

A COMPARISON OF EXPERIMENTAL AND COMPUTED LATERAL LOAD DISTRIBUTION FOR TWO CONTINUOUS STEEL GIRDER HIGHWAY BRIDGES

A Thesis

Presented for the

Master of Science

Degree

The University of Tennessee

Edwin A. McDougle, Jr.

December 1975

1266317

ABSTRACT

Four deck girder highway bridges in Tennessee, located in an area which has since been inundated as a part of the Tennessee Valley Authority Tims Ford Reservoir, were tested under rolling loads utilizing an HS-20 vehicle (72,000 pounds), an overloaded HS-20 vehicle (132,500 pounds), an M-60 combat tank (105,000 pounds), and an HET-70 tank transporter (195,400 pounds). The bridges were then tested with static loads to failure. Research was directed toward evaluation of existing design criteria.

This thesis is concerned in particular with the measured lateral distribution of load from working loads to first yield of steel for two of the four bridges tested. Both of the subject bridges were multi-span continuous steel girder, concrete deck bridges. The results are compared with three empirical methods and one theoretical method of analysis.

A consideration of test results and their comparison with empirical and theoretical results permits the following conclusions to be drawn:

(1) The lateral distribution of load was found to be pratically independent of load level up to first yield of the steel.

(2) The AASHTO specifications require distribution factors which are conservative for interior girders and unconservative for exterior girders, indicating that they do

not account for the additional stiffness contributed to the exterior girder by curbs and handrails.

(3) The theoretical research on box beam bridges by Motarjemi and Van Horn at Lehigh University should be extended to steel girder bridges and compared to the results herein.

(4) Finite element models of bridges are a powerful tool in predicting total bridge behavior, including lateral distribution of load, but great care should be taken in defining the model to insure that it acts like the real structure.

(5) AASHTO requirements predicted the distribution factors as well as the other methods reported herein.

TABLE OF CONTENTS

CHAPTER		PAGE
I.	INTRODUCTION	1
	Background Information	1
	Objective of Thesis	2
	Description of Bridges	3
II.	DESCRIPTION OF ROLLING LOAD TESTS	8
	Description of Test Vehicles	8
	FHWA Test Vehicle	8
	U. T. Test Vehicle	8
	Army M-60 Tank	8
	Army HET-70 Transporter	11
	Outline of Tests	11
	Bridge 1	11
	Bridge 4	13
III.	DESCRIPTION OF STATIC TESTS TO FAILURE	17
	Placement of Load	17
	Bridge 1	17
	Bridge 4	17
	Application of Loads	20
	Rock Anchor System	20
	Bearing Grill	20
	Loading Procedure	21
IV.	LATERAL LOAD DISTRIBUTION - EXPERIMENTAL DATA AND RESULTS	22
	Instrumentation	22

CHAPTER PAGE

Method of Data Interpretation. 22
Bridge 1 24
Bridge 4 24
Results. 25
Rolling Load Tests - Bridge 1. 25
Rolling Load Tests - Bridge 4. 25
Static Load Tests - Bridge 1 25
Static Load Tests - Bridge 4 46
V. PREDICTION OF LATERAL DISTRIBUTION 50
Explanation of Distribution Methods. 50
AASHTO Specifications. 50
Sanders and Elleby Proposal. 51
Motarjemi and Van Horn Recommendations . . 52
STRUDL II Analyses 53
Rolling Load Test Results. 54
Distribution Factors - Bridge 1. 57
AASHTO Specifications. 57
Sanders and Elleby Proposal. 57
Motarjemi and Van Horn Recommendations . . 58
STRUDL II Analysis 59
Rolling Load Test Results. 59
Distribution Factors - Bridge 4. 62
AASHTO Specifications. 62
Sanders and Elleby Proposal. 62
Motarjemi and Van Horn Recommendations . . 62

CHAPTER PAGE

STRUDL II Analysis 63

Rolling Load Test Results. 63

VI. DISCUSSION 66

Rolling Load Tests 66

Discussion of Actual and Theoretical

Distribution Factors 66

Test Results 67

AASHTO Specifications. 67

Sanders and Elleby Proposal. 70

Motarjemi and Van Horn 71

STRUDL II Analyses 72

Static Load Tests to Failure 73

VII. CONCLUSIONS. 75

LIST OF REFERENCES 77

VITA 80

LIST OF TABLES

TABLE		PAGE
1.	Description of Bridges.	4
2.	Summary of Rolling Load Tests - Bridge 1. . . .	14
3.	Summary of Rolling Load Tests - Bridge 4. . . .	16
4.	Load Distribution Coefficients - Bridge 1 Rolling Load Tests.	26
5.	Load Distribution Coefficients - Bridge 4 Rolling Load Tests.	34
6.	Load Distribution Coefficients - Bridge 1 Static Load Tests to Failure.	45
7.	Load Distribution Coefficients - Bridge 4 Static Load Tests to Failure.	47
8.	Comparison of Distribution Factors for Bridge 1	61
9.	Comparison of Distribution Factors for Bridge 4	65

LIST OF FIGURES

FIGURE		PAGE
1.	Photographs of Bridges 1 and 4.	5
2.	Cross-Section of Bridge No. 1	6
3.	Cross-Section of Bridge No. 4	7
4.	Diagram of HS-20 Test Vehicle	9
5.	Diagram of HS-40 Test Vehicle	10
6.	Diagram of HET-70 Tank Transporter.	12
7.	Position of Loads for Static Tests to Failure - Bridge No. 1.	18
8.	Position of Loads for Static Tests to Failure - Bridge No. 4.	19
9.	Strain Gage Locations at Section A-A.	23
10.	Distribution Coefficients for HS-40 Truck in Lanes 1, 2, and 3	27
11.	Distribution Coefficients for HS-40 Truck Moving Forward with HS-20 Truck Following Backward at Crawl Speed	28
12.	Distribution Coefficients for HS-20 Truck and HS-40 Truck in Lanes 1 and 3 Simultaneously .	29
13.	Distribution Coefficients for M-60 Tank in Lanes 2 and 3	30
14.	Distribution Coefficients for HET-70 Transporter in Lanes 2 and 3.	31

FIGURE PAGE

15. Comparison of Distribution Coefficients for Different Vehicles (or Combinations) in Lane 2. 32

16. Comparison of Distribution Coefficients for Different Vehicles (or Combinations) in Lane 3. 33

17. Distribution Coefficients for HS-40 Truck in Lanes 1, 2, and 3 Travelling Southbound . . . 35

18. Distribution Coefficients for HS-40 Truck in Lanes 1, 2, and 3 Travelling Northbound . . . 36

19. Distribution Coefficients for HS-40 Truck in Lanes 1 and 2 Travelling at 10 MPH. 37

20. Distribution Coefficients for HS-40 Truck in Lanes 1 and 2 Travelling at 20 MPH. 38

21. Distribution Coefficients for HS-20 Truck in Lanes 1, 2, and 3 39

22. Comparison of Distribution Coefficients for HS-40 Truck in Lane 1 Travelling at Crawl Speed, 10 MPH, and 20 MPH 40

23. Comparison of Distribution Coefficients for HS-40 Truck in Lane 2 Travelling at Crawl Speed, 10 MPH, and 20 MPH 41

24. Comparison of Distribution Coefficients for HS-40 and HS-20 Trucks in Lane 1. 42

FIGURE PAGE

25. Comparison of Distribution Coefficients for HS-40 and HS-20 Trucks in Lane 2. 43

26. Comparison of Distribution Coefficients for HS-40 and HS-20 Trucks in Lane 3. 44

27. Distribution Coefficients for Static Tests to Failure with Loads at Points A and B Only . . 48

28. Distribution Coefficients for Static Tests to Failure with Loads at Points C, D, E, and F . 49

29. Load Distribution Coefficient Influence Lines for a Single HS-40 Vehicle on Bridge 1. . . . 55

30. Load Distribution Coefficient Influence Lines for a Single HS-40 Vehicle on Bridge 4. . . . 56

31. Comparison of Actual and Theoretical Distribution Factors for Bridge 1 68

32. Comparison of Actual and Theoretical Distribution Factors for Bridge 4 69

CHAPTER I

INTRODUCTION

Background Information

Three Tennessee State Highway bridges and one Franklin County Highway bridge were located in an area which has since been inundated as a part of the Tennessee Valley Authority's Tims Ford Reservoir. These bridges were made available by the TVA, the Tennessee Department of Highways, and the Franklin County Highway Department for testing purposes. The availability of four highway bridges, each designed according to the American Association of State Highway Officials (AASHO) Specifications current at the time, presented a truly unique opportunity to compare design criteria with actual bridge behavior over the full range of moving working loads as well as static loads to ultimate.

During the period between April 18 and May 8, 1969, the Bureau of Public Roads in cooperation with the Tennessee Department of Highways, the Department of the Army, and the University of Tennessee performed numerous rolling load tests on three of the bridges using the M-60 combat tank and the HET-70 tank transporter. The purpose of these tests was to determine the actual live load moment distribution for various moving live loads to the main beams for correlations with empirical design distributions (from AASHO) and with the distributions presented by analytical methods (1).

On January 1, 1970, a contract was executed between the University of Tennessee and the Tennessee Department of Highways in cooperation with the Federal Highway Administration for conducting full-scale load tests on all of the bridges to determine the lateral distribution of load, the dynamic response, the ultimate strength, and the mode of failure. These tests were performed during the summer of 1970 (2).

Objective of Thesis

This thesis will describe the experimental methods used and the results obtained as a part of the University of Tennessee's full-scale bridge testing program (FSBT) and the Bureau of Public Roads tank transporter tests to determine the lateral distribution of load on two multi-span continuous steel beam and slab highway bridges.

The results of an ICES STRUDL II finite element analysis relating to lateral load distribution for each bridge (3,4) will be discussed and compared with the experimental results from FSBT. Both the analytical and experimental results will then be compared to the empirical design equation in the 1973 AASHO Specifications (5) and the proposed revisions to the AASHO Specifications made by Sanders and Elleby (6) and Motarjemi and Van Horn (7).

Description of Bridges

Each of the four bridges tested in the Full Scale Bridge Test (FSBT) program was a two-lane deck girder bridge with four longitudinal girders. The Bureau of Public Roads (BPR) tests were performed on three of these four bridges. The findings reported in this thesis are limited to two of the FSBT bridges, which include one of the BPR bridges. These bridges are numbered 1 and 4 in the FSBT Final Report (2) and will be so referenced in this thesis. A description of the bridges is given in Table 1, and photographs of the bridges are shown in Figure 1. Cross sections of both bridges are shown in Figures 2 and 3.

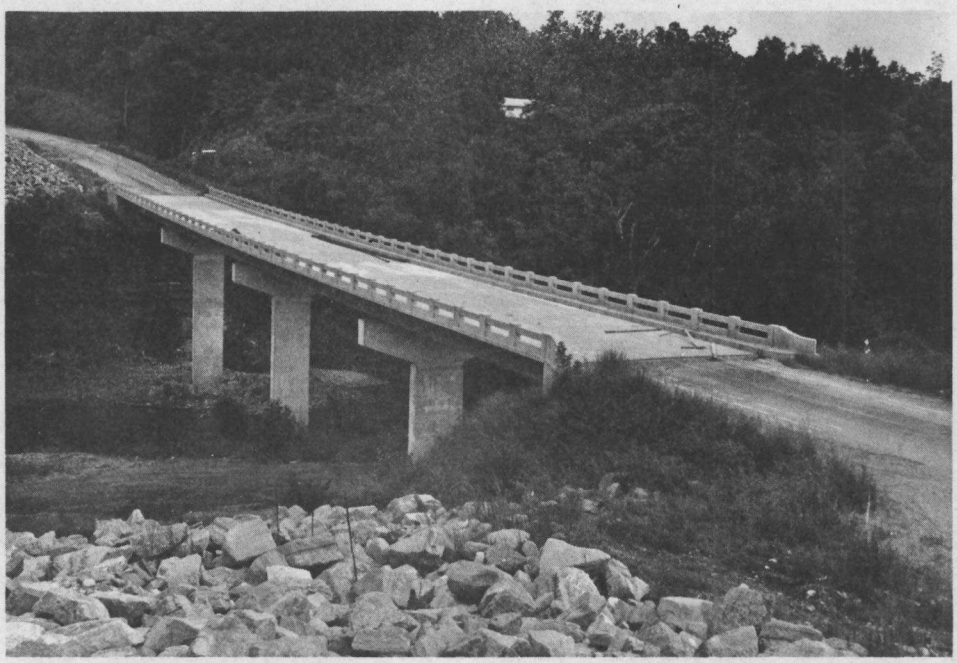
Bridge 1 was on a flat sag vertical curve, but in all other respects these two bridges were ideal for testing: 90° skew, horizontal tangent, almost zero grade, and recent construction.

Both of the bridges appeared to be structurally sound prior to testing. Approximate "Average Daily Traffic" volumes in 1968 for Bridges 1 and 4 were 600 and 200 respectively.

TABLE 1

DESCRIPTION OF BRIDGES

Bridge Number	General Description	Span	Girder Spacing	Skew	Location	Loading and Date
1	4-Span Continuous, 36" Steel Rolled Beams Composite in Positive Moment Regions	70'-90'-90'-70'	8'-4"	90°	Tenn. Rt. 130 over Elk River	HS-20 1963
4	3-Span Continuous, Non-Composite, 27" Steel Rolled Beams	45'-60'-45'	7'-4"	90°	Mansford Road over Elk River	HS-15 1956



(a) BRIDGE 1



(b) BRIDGE 4

FIGURE 1. PHOTOGRAPHS OF BRIDGES 1 AND 4

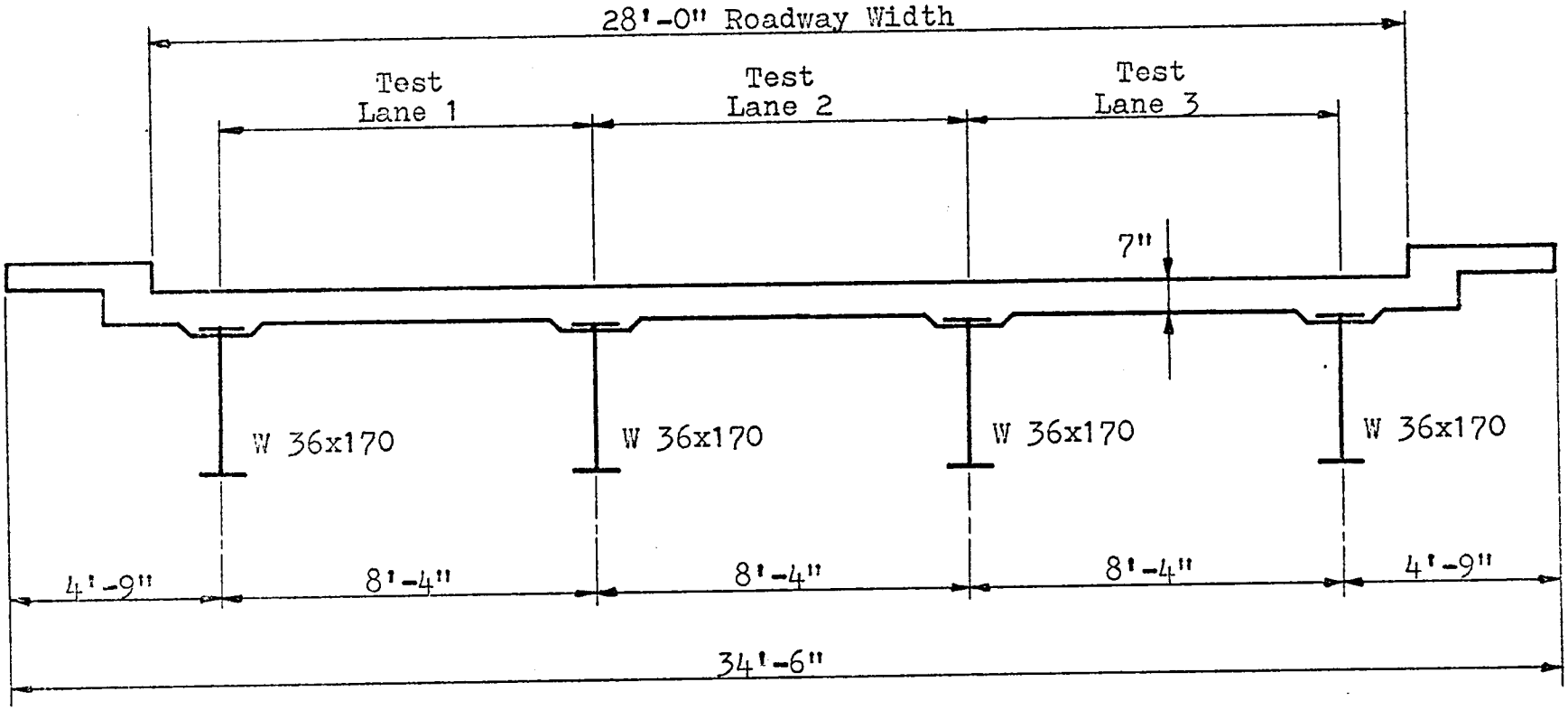


FIGURE 2. CROSS-SECTION OF BRIDGE NO. 1

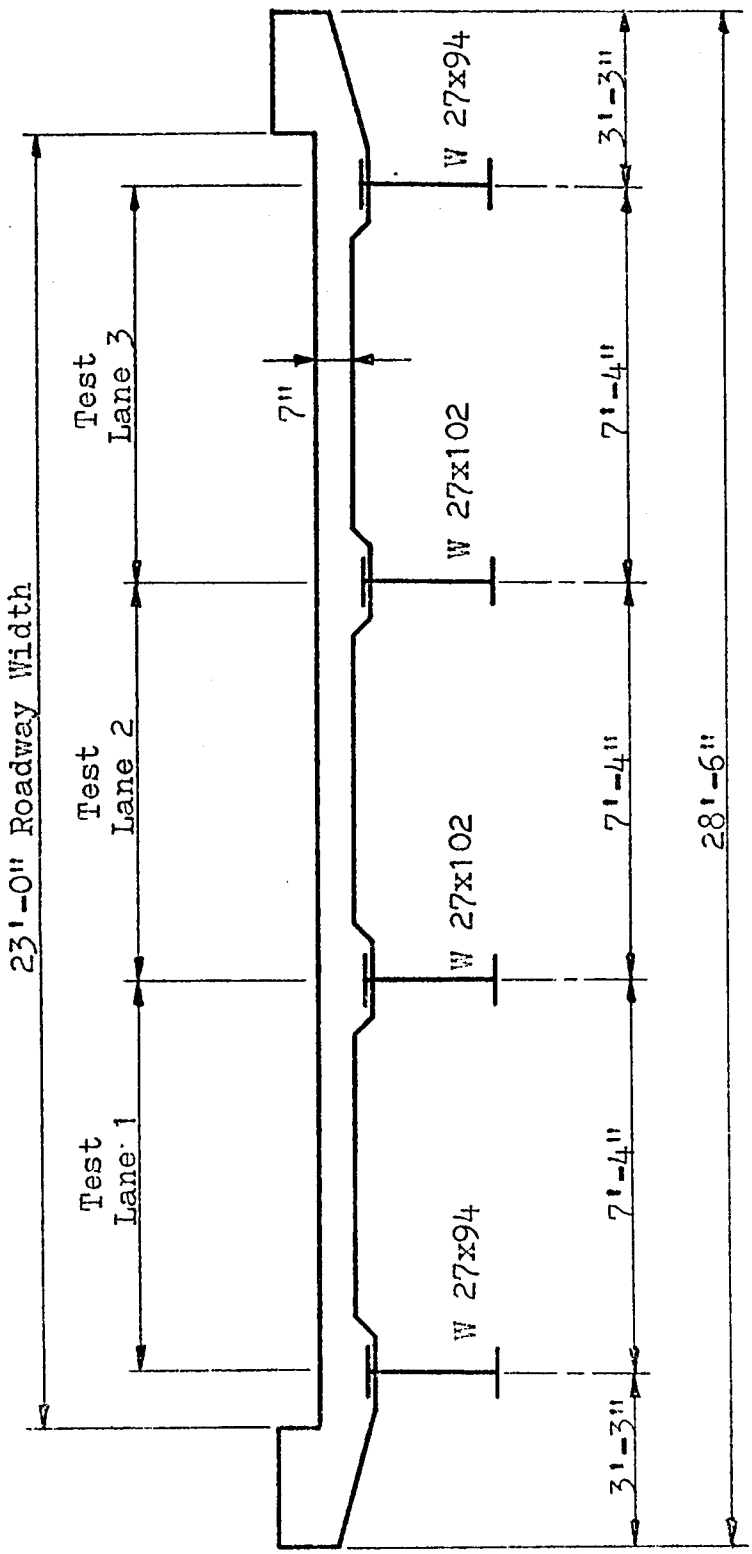


FIGURE 3. CROSS-SECTION OF BRIDGE NO. 4

CHAPTER II

DESCRIPTION OF ROLLING LOAD TESTS

In order to determine the lateral distribution of applied rolling loads, four different vehicles were driven across the bridges in each of three test lanes at speeds ranging from crawl to 35 mph.

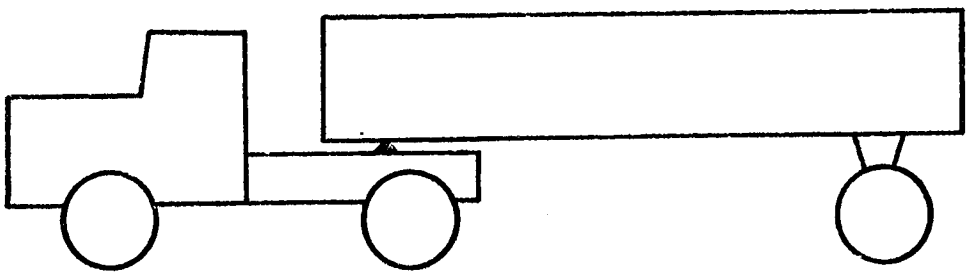
Description of Test Vehicles

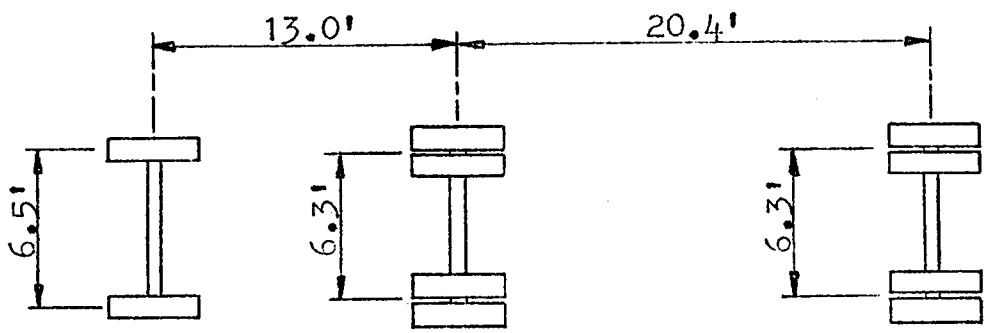
The vehicles used to load the bridges included the Federal Highway Administration Test Vehicle, the University of Tennessee Test Vehicle, the Army M-60 track-laying combat tank, and the Army HET-70 tank transporter.

FHWA Test Vehicle. This vehicle, hereinafter referred to as "HS-20," is a tractor and semitrailer combination which when loaded to 72,000 pounds closely simulates the HS-20 design vehicle loading. Wheel spacing, axle spacing, and loads are shown in Figure 4. Truck loading was accomplished with solid concrete blocks on pallets.

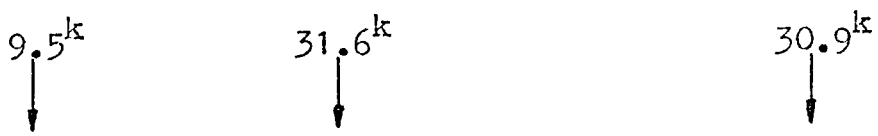
U. T. Test Vehicle. This vehicle, hereinafter referred to as "HS-40," is a tractor and flat bed semitrailer combination which when loaded to 132,500 pounds with solid concrete blocks on pallets has axle loads almost double those allowed by the HS-20 design load. Wheel spacing, axle spacing, and loads are shown in Figure 5.

Army M-60 Tank. The M-60 track-laying combat tank weighs approximately 105,000 pounds. This weight is carried



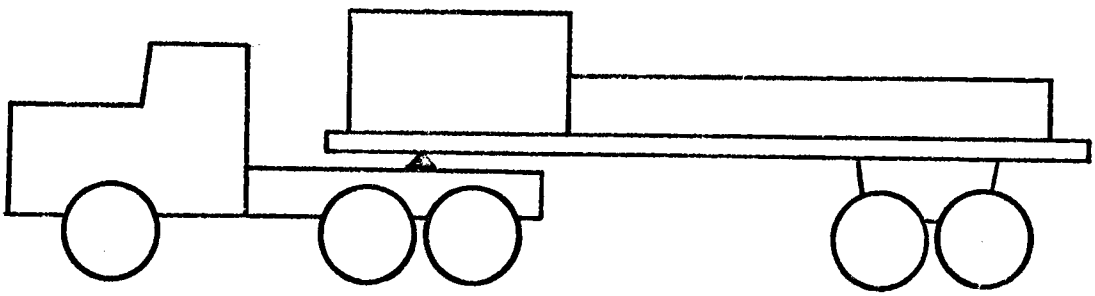


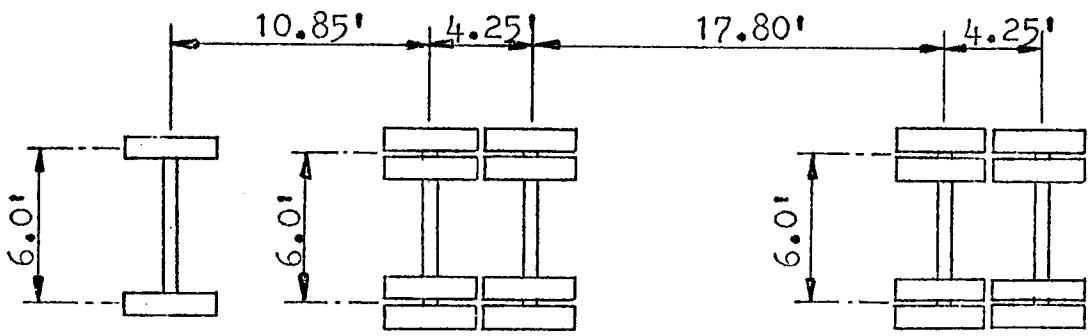
AXLE AND WHEEL SPACING



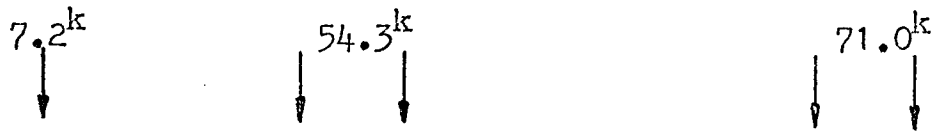
AXLE LOADS

FIGURE 4. DIAGRAM OF HS-20 TEST VEHICLE





AXLE AND WHEEL SPACING



AXLE LOADS

FIGURE 5. DIAGRAM OF HS-40 TEST VEHICLE

on two 22 inch wide rubber-cleated tracks at 9.5 foot centers. The tracks contact the roadway over a 14 foot length.

Army HET-70 Transporter. This vehicle has eight pneumatic-tired axles with a fully loaded gross load of 195,400 pounds. This results when the transporter is carrying an MBT-70 battle tank and was obtained by loading the transporter with an M-60 combat tank with a surcharge of armor plate strapped to the tank body. The HET-70 has a total vehicle width of 12 feet and the dual wheels of the four rear axles are at 8'-6" centers. Axle spacings and loads are shown in Figure 6.

Outline of Tests

The rolling load tests outlined here are those upon which the results and conclusions discussed later herein are based. The vehicles previously described were utilized alone and in various combinations together on the bridges for 34 tests with variables including the speed and lane position. A more detailed description of the various tests for each bridge is given below.

Bridge 1. A total of twelve tests were conducted utilizing the HS-40 loading alone for seven tests and in conjunction with the HS-20 loading for five tests. All of the tests were with the vehicles headed south as they crossed the bridge. The HS-40 loading was used at crawl speed in the right lane and center lane positions twice and in the left

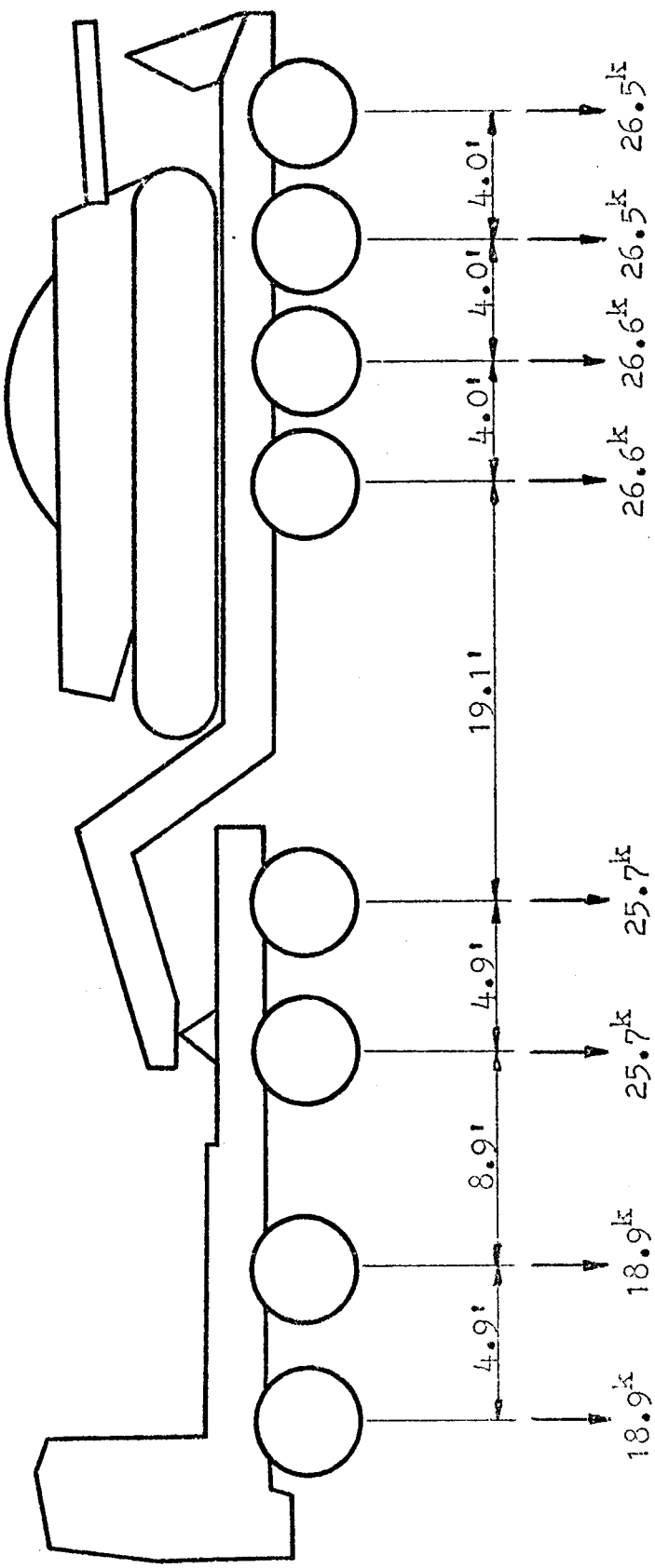


FIGURE 6. DIAGRAM OF HET-70 TANK TRANSPORTER

lane once. A nominal speed of 35 mph was used for two tests with the vehicle in the right and center lanes. The HS-40 and HS-20 were positioned side by side and crossed the bridge at crawl speed. The lane positions of the two trucks were reversed, and the test was repeated. In order to simulate the heaviest lane loading, the HS-40 vehicle was driven across the bridge with the HS-20 vehicle following closely behind travelling backwards. This loading was used for three tests using the three lane positions.

The M-60 and HET-70 vehicles crossed the bridge individually in each of the three lanes moving northbound and southbound. Table 2 summarizes the rolling load tests for Bridge 1.

Bridge 4. A total of fifteen tests were conducted utilizing the HS-20 and HS-40 vehicle loadings. All of the crossings except three were in the northbound direction. The HS-40 vehicle was used for three tests with the vehicle in the right, center, and left lanes travelling northbound at crawl speed. Three southbound crossings were made with the HS-40 and HS-20 vehicles individually at crawl speed for a total of six tests. Higher speed runs were made with the HS-40 vehicle in the left and center lanes. The HS-40 and HS-20 vehicles were used side by side at crawl speed. The lane positions of the two trucks were reversed, and the test was repeated.

TABLE 2

SUMMARY OF ROLLING LOAD TESTS - BRIDGE 1

Test Vehicle	Lane Number	Speed
HS-40	1	Crawl
HS-40	2	Crawl
HS-40	2	Crawl
HS-40	3	Crawl
HS-40	3	Crawl
HS-40	2	35 mph
HS-40 forward HS-20 backward	1	Crawl
HS-40 forward HS-20 backward	2	Crawl
HS-40 forward HS-20 backward	3	Crawl
HS-20 HS-40	1 3	Crawl
HS-40 HS-20	1 3	Crawl
M-60 tank	1	Crawl
M-60 tank	2	Crawl
M-60 tank	3	Crawl
HET-70 transporter	1	Crawl
HET-70 transporter	2	Crawl
HET-70 transporter	3	Crawl

There were no M-60 combat tank or HET-70 tank transporter load tests performed on this bridge. Table 3 summarizes the rolling load tests for Bridge 4.

TABLE 3

SUMMARY OF ROLLING LOAD TESTS - BRIDGE 4

Test Vehicle	Lane Number	Direction of Travel	Speed
HS-40	1	Southbound	Crawl
HS-40	2	Southbound	Crawl
HS-40	3	Southbound	Crawl
HS-40	1	Southbound	10 mph
HS-40	2	Southbound	10 mph
HS-40	3	Southbound	10 mph
HS-40	1	Southbound	20 mph
HS-40	2	Southbound	20 mph
HS-40	3	Southbound	20 mph
HS-40	1	Northbound	Crawl
HS-40	2	Northbound	Crawl
HS-40	3	Northbound	Crawl
HS-20	1	Southbound	Crawl
HS-20	2	Southbound	Crawl
HS-20	3	Southbound	Crawl

CHAPTER III

DESCRIPTION OF STATIC LOAD TESTS TO FAILURE

In order to determine the lateral distribution of loads at high load levels and how the distribution changes with increasing load, static tests to failure were performed on each bridge.

Placement of Load

Bridge 1. The loads were placed on this bridge in such a way as to simulate an HS truck in each lane, located in the approximate position to cause maximum positive moment near the center of the span. The points on the span at which load was applied were at the positions of the eight rear wheels of the two simulated trucks. For the test to failure, the four front wheels were simulated by four 4,000 pound pallets of concrete blocks. The positions of the applied loads for Bridge 1 are illustrated in Figure 7.

Bridge 4. The load placement for this bridge was originally intended to be similar to that described above for Bridge 1; however, because of difficulties in rock drilling, only six load points were used. The simulation of front wheels was omitted for this bridge because they had little effect on the results for Bridge 1. The positions of the applied loads for Bridge 4 are shown in Figure 8.

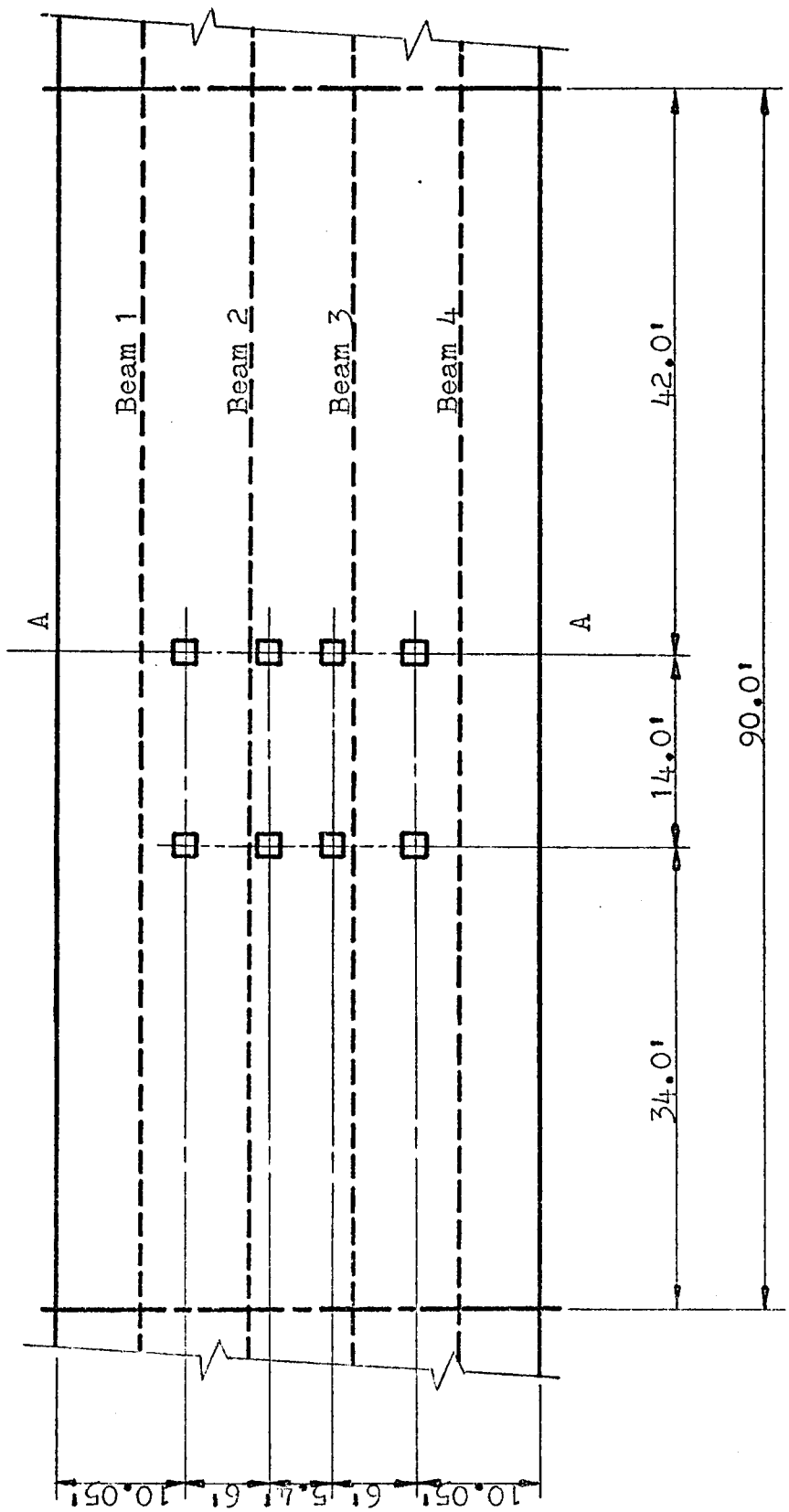


FIGURE 7. POSITION OF LOADS FOR STATIC TESTS TO FAILURE - BRIDGE NO. 1

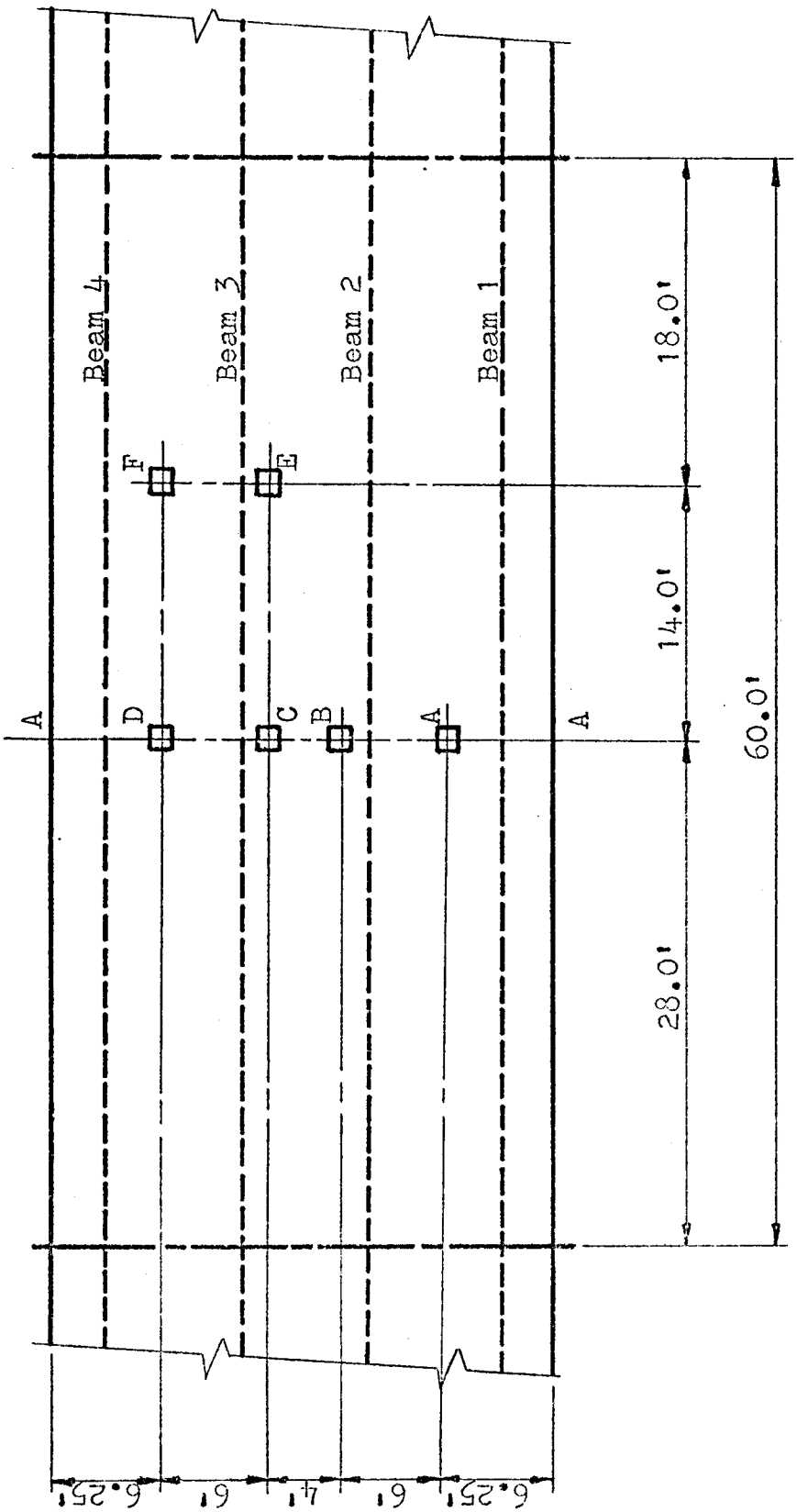


FIGURE 8. POSITION OF LOADS FOR STATIC TESTS TO FAILURE - BRIDGE NO. 4

Application of Loads

The large loads used in the static tests were developed through a "rock anchor" system and were applied to the bridge deck through a "bearing grill."

Rock Anchor System. At each of the load points for both bridges a hole was drilled through the concrete bridge deck. Directly below each one of these holes, a hole was drilled approximately twenty-five feet into the limestone rock, and an 18S reinforcing bar was grouted into place in this hole. The bar was terminated below the bridge deck, and a $1\frac{3}{8}$ in. diameter Stressteel bar was connected to the 18S bar with a connection designed by the reseachers. The Stressteel bar extended through the hole in the bridge deck and through a 100 ton capacity center-hole jack, which rested on a "bearing grill."

Bearing Grill. The bearing grill consisted of two fourteen in. wide flange beams, 3 ft.-10 in. long, spaced two feet - six inches center to center. These beams were joined at the ends by two 12 in. channels, which spanned between the beams and were welded to the beams so that the bottom flanges of the channels were flush with the bottom surfaces of the beams in order to obtain uniform bearing. Two more channels spanned between the beams at the center of their 3 ft. - 10 in. length and were fastened to the beam webs. The load was applied by the hydraulic rams through a two inch thick steel bearing plate to these center channels.

Soft wood 2 in. x 10 in.'s were placed under the beams and on the bridge deck, and 2 in. x 4 in.'s were placed under the end channels in order to minimize stress concentrations and reduce the likelihood of a punching shear failure in the bridge deck.

Loading Procedure

The load was applied to each load point by a Stressteel center-hole ram acting on a bearing grill. Each ram had a six inch stroke. Grip nuts were used in most of the tests to permit the bridge deflection attained in one stroke to be held while the rams were reset. The rams were activated by hydraulic pressure from an electric pump equipped with a pressure gage which had a maximum capacity of 10,000 p.s.i. The loads were applied in increments of 1,000 p.s.i. up to near yielding and then in increments of 500 p.s.i. which corresponded to approximately 10 kips per ram. The force in each Stressteel bar was obtained from strain readings after each load increment. Also, in order to determine load distribution to the main beams, strains at various points in the bridge were monitored.

The tests were discontinued at some point after the ultimate load of the bridges was obtained. Ultimate load is defined as the maximum load attained in a test to "failure," and "failure" was said to have occured when an increase in deflection of the bridge took place under a decreasing load.

CHAPTER IV

LATERAL LOAD DISTRIBUTION - EXPERIMENTAL DATA AND RESULTS

The lateral distribution of loads is determined by the bending moment supported by each girder due to a particular loading condition. The bending moment in each girder is computed utilizing the measured strain in the top and bottom fibers in combination with the properties of the girder cross-section.

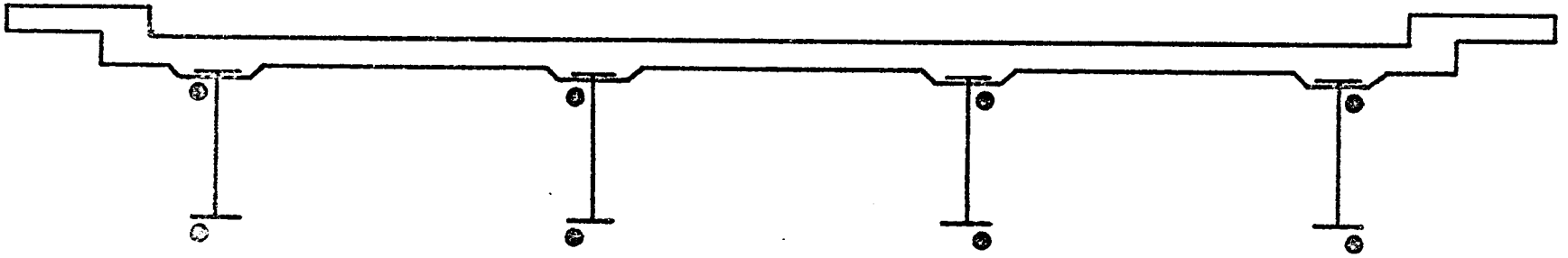
Instrumentation

For the determination of lateral distribution of loads each of the four girders had a foil gage mounted on the underside of their top and bottom flanges. Micromeasurements type EA-06-250BG-120 gages having a resistance of 120 ohms and a gage factor of 2.11 were used. Figure 9 shows the location of strain gages at Section A-A of each bridge.

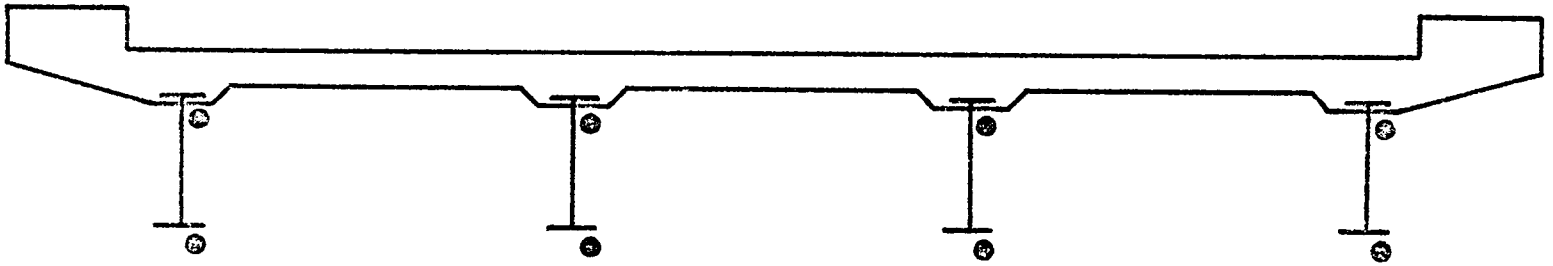
A Budd model HW-1 strain indicator model SB-1 switch and balance unit was used to monitor the strains in the foil gages mounted on the Stressteel bars. These strains were used to determine the load on the bridge at any time during the static tests to failure.

Method of Data Interpretation

From the measured strains in the top and bottom flanges, the moment in each individual girder was computed.



(a) BRIDGE 1



(b) BRIDGE 4

● - denotes strain gage

FIGURE 9. STRAIN GAGE LOCATIONS AT SECTION A-A

Bridge 1. This bridge was designed and constructed to act compositely in positive moment regions. From the strains at Section A-A the neutral axis of the composite section was located. Based on the neutral axis location, the centroid of the compressive force in the slab could be located quite accurately for both interior and exterior girders. The magnitude of the tensile force was calculated from the known stress-strain properties of the steel, and the moment was calculated as the product of the tensile force and the moment arm of the interal couple.

Bridge 4. This bridge was designed to act non-compositely; however, the experimentally located position of the neutral axis clearly indicated that a considerable degree of composite action did exist. Additional strain gage information also verified the interaction between the slab and beams. From the measured strains the neutral axis was located, and the location of the resultant compressive force for each girder section could be estimated closely. The total tensile force was calculated from the measured strains and the known stress-strain properties of the steel, and the moment for each girder was calculated as the product of the tensile force and the moment arm of the internal couple.

The sum of the moments for the four girders was obtained for each static loading condition on each bridge and compared to the moment calculated using the STRUDL - II subset of the ICES computer program. The experimental and

calculated moments were in consistent agreement, which indicated that the moment arm of the internal couple was sufficiently accurate.

Results

The term, "Load Distribution Coefficient," is used herein to denote the percentage of total live load bending moment supported by a particular longitudinal girder.

Rolling Load Tests - Bridge 1. The coefficients in Table 4 indicate the lateral distribution of load on Bridge 1 due to the HS-40 vehicle, the HS-20 vehicle, the HS-40 combined with the HS-20 vehicle, the M-60 battle tank, and the HET-70 transporter. Figures 10 through 14 graphically illustrate these same coefficients. Figures 15 and 16 show a direct comparison of the distribution coefficients for four different vehicles (or combinations of vehicles) in lanes 2 and 3 respectively.

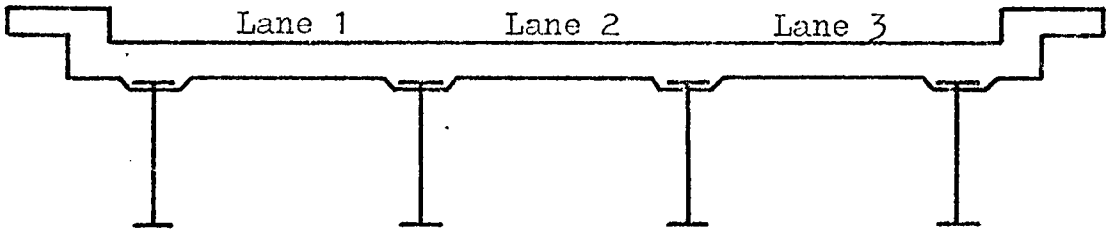
Rolling Load Tests - Bridge 4. The coefficients indicating the lateral distribution of load on Bridge 4 due to the HS-40 vehicle and the HS-20 vehicle are listed in Table 5. Figures 17 through 21 graphically illustrate these coefficients. Figures 22 through 26 show a direct comparison of distribution coefficients for various combinations of vehicles, speeds, and direction for each of the three lanes.

Static Load Tests - Bridge 1. The coefficients in Table 6 indicate the lateral distribution of load on Bridge 1

TABLE 4

LOAD DISTRIBUTION COEFFICIENTS - BRIDGE 1
ROLLING LOAD TESTS

Test Vehicle	Lane Number	Vehicle Speed	Distribution Coefficients, % 1	2	3	4
HS-40	1	Crawl	46	37	16	2
HS-40	2	Crawl	20	32	29	19
HS-40	2	Crawl	16	33	31	19
HS-40	3	Crawl	2	17	36	45
HS-40	3	Crawl	2	16	35	47
HS-40	2	35 mph	20	30	32	18
HS-40 HS-20	1	Crawl	40	40	17	3
HS-40 HS-20	2	Crawl	20	31	29	20
HS-40 HS-20	3	Crawl	2	14	34	50
HS-20 HS-40	1 3	Crawl	18	24	27	31
HS-40 HS-20	1 3	Crawl	29	30	23	18
M-60	1	Crawl	49	32	16	3
M-60	2	Crawl	21	31	29	19
M-60	3	Crawl	3	16	32	49
HET-70	1	Crawl	49	32	15	4
HET-70	2	Crawl	22	29	28	21
HET-70	3	Crawl	4	15	32	49



BRIDGE 1

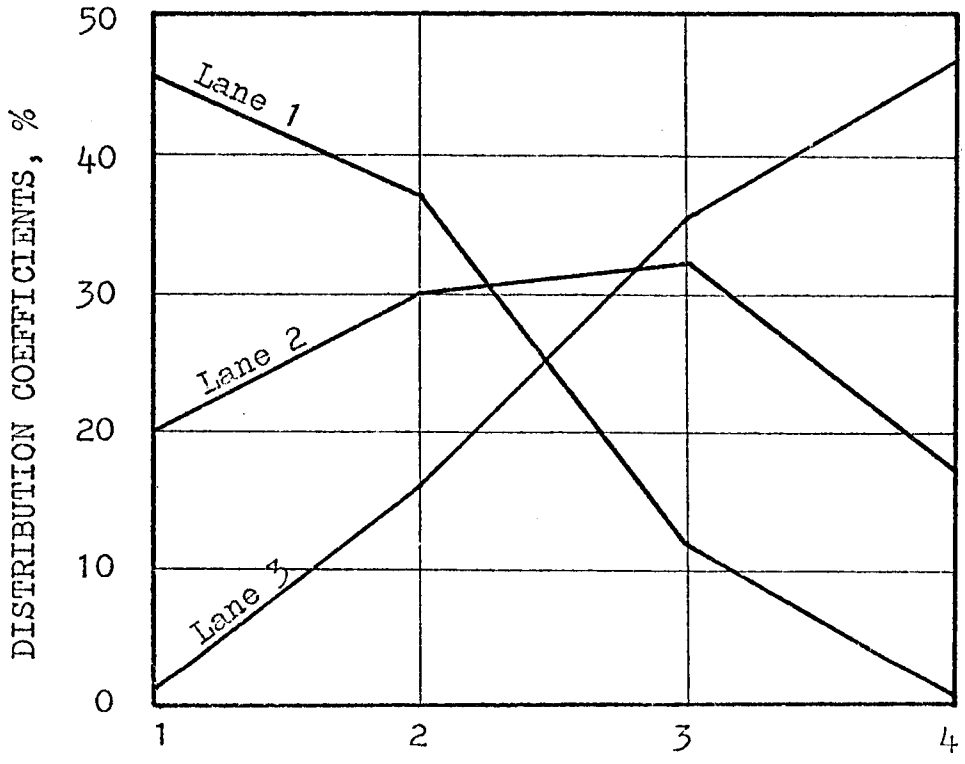
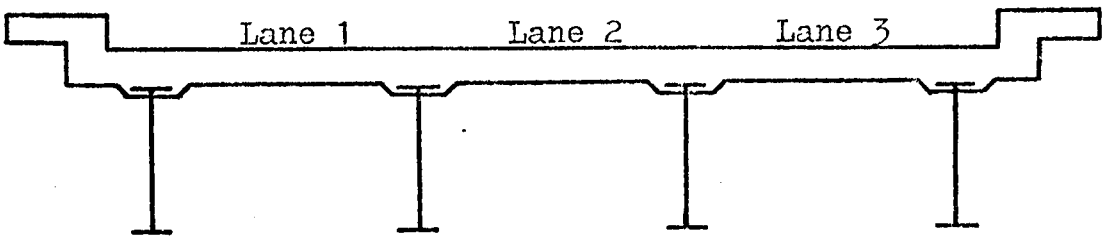


FIGURE 10. DISTRIBUTION COEFFICIENTS FOR HS-40 TRUCK IN LANES 1, 2, AND 3



BRIDGE 1

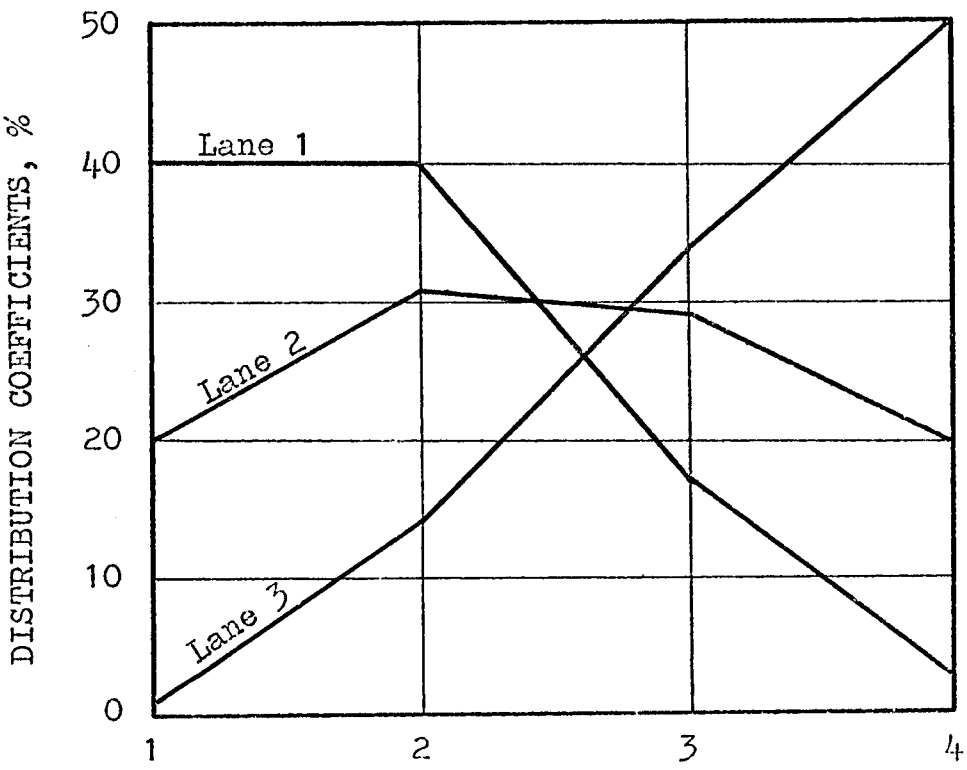
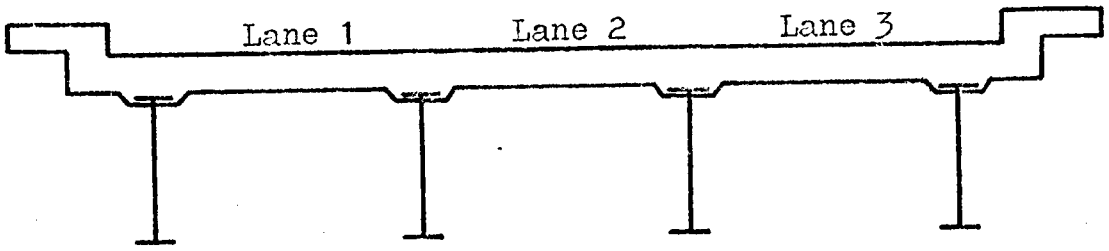


FIGURE 11. DISTRIBUTION COEFFICIENTS FOR HS-40 TRUCK MOVING FORWARD WITH HS-20 TRUCK FOLLOWING BACKWARD AT CRAWL SPEED



BRIDGE 1

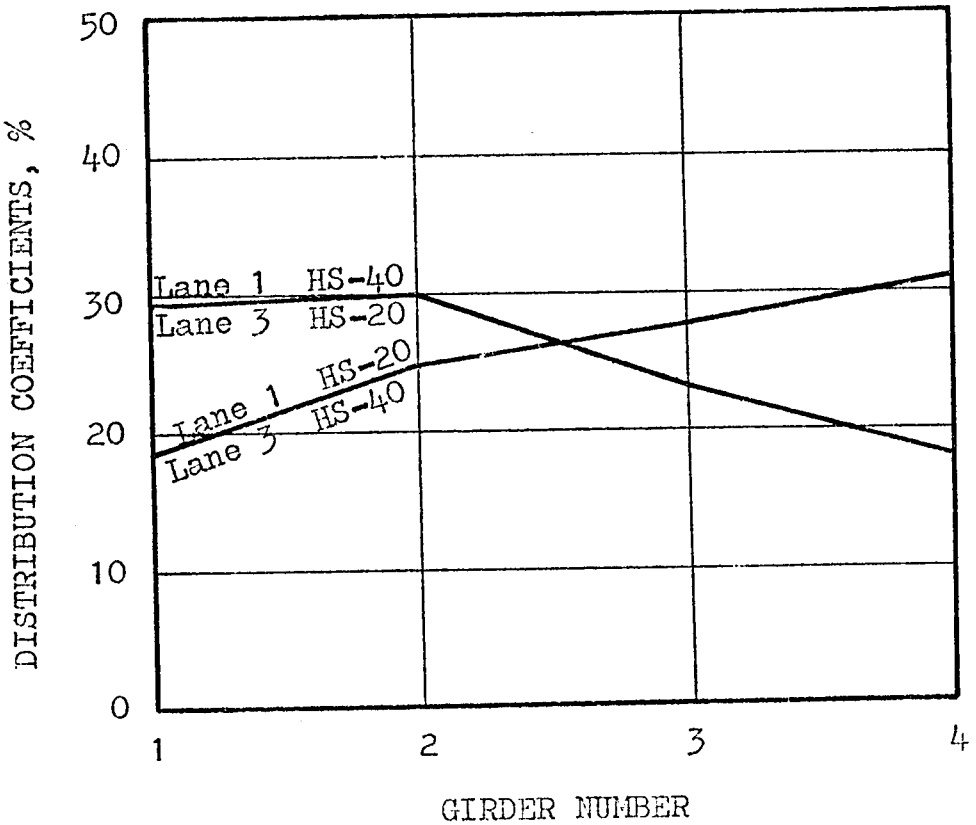
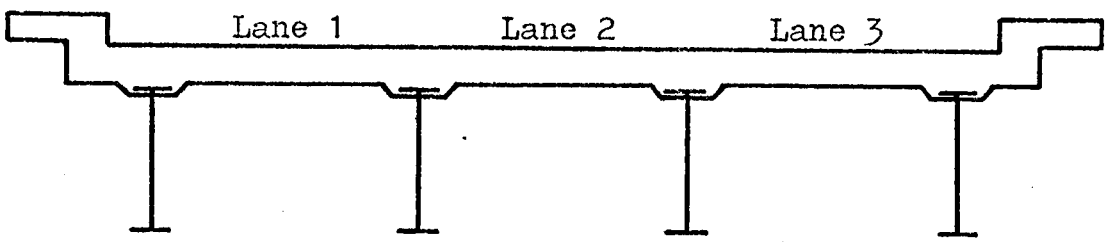


FIGURE 12. DISTRIBUTION COEFFICIENTS FOR HS-20 TRUCK AND HS-40 TRUCK IN LANES 1 AND 3 SIMULTANEOUSLY



BRIDGE 1

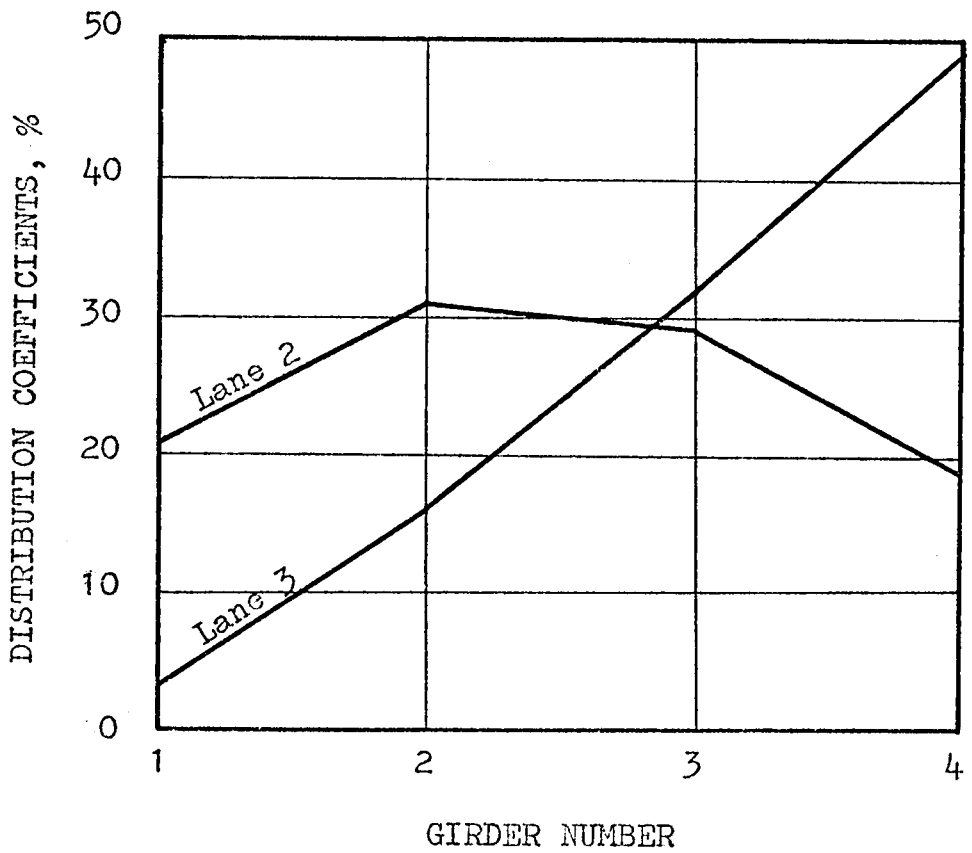
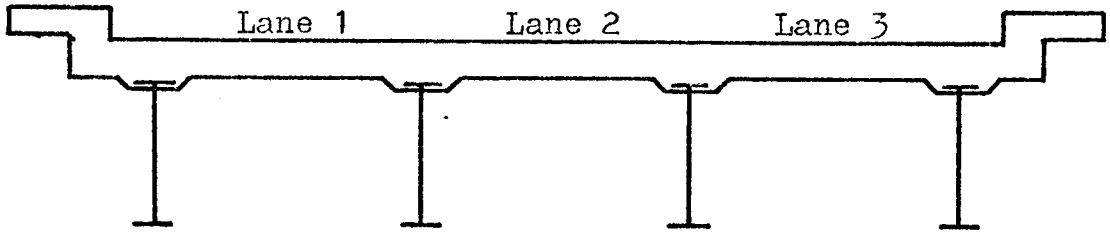


FIGURE 13. DISTRIBUTION COEFFICIENTS FOR M-60 TANK IN LANES 2 AND 3



BRIDGE 1

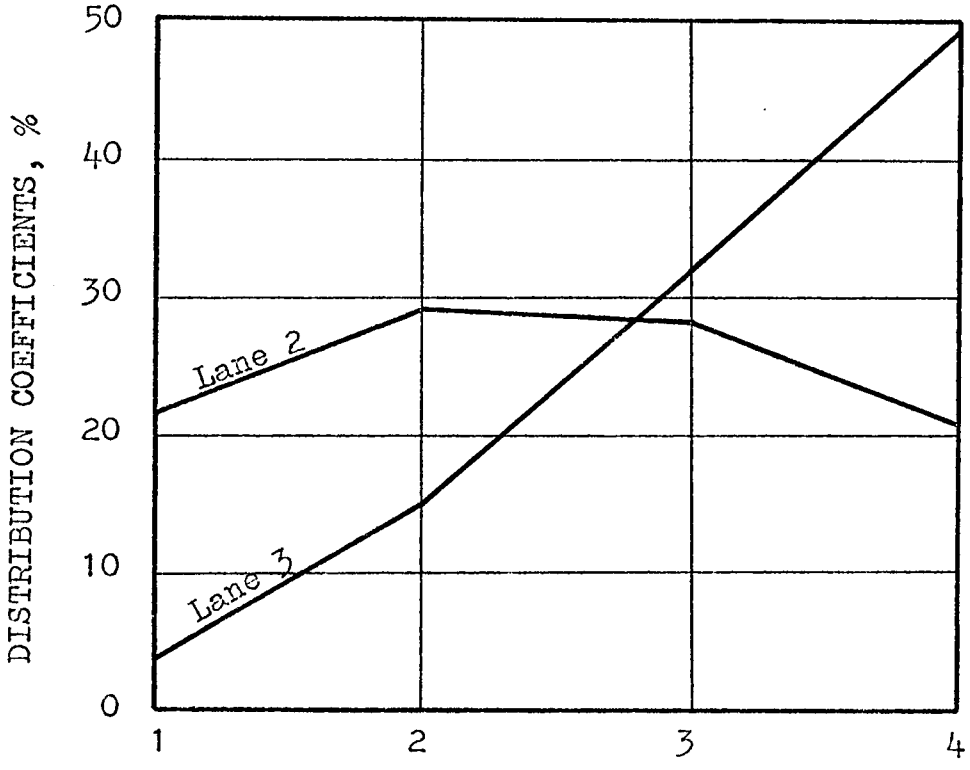
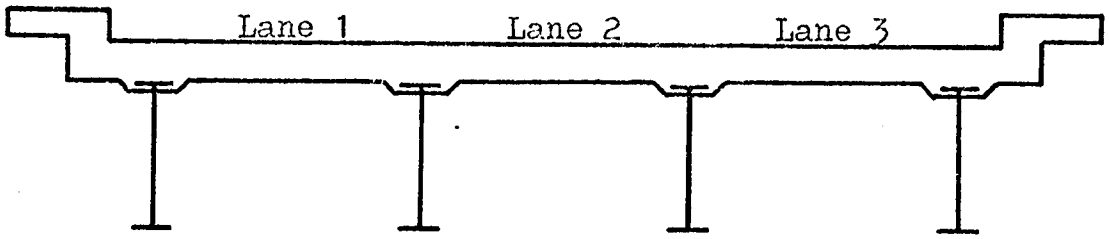


FIGURE 14. DISTRIBUTION COEFFICIENTS FOR HET-70 TRANSPORTER IN LANES 2 AND 3



BRIDGE 1

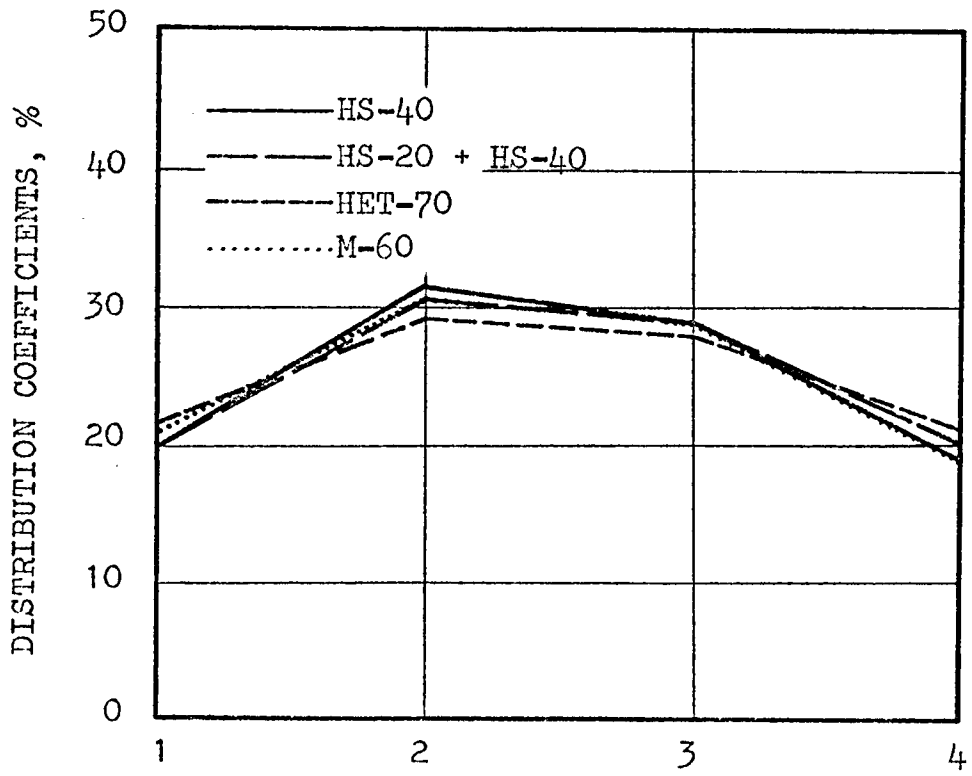
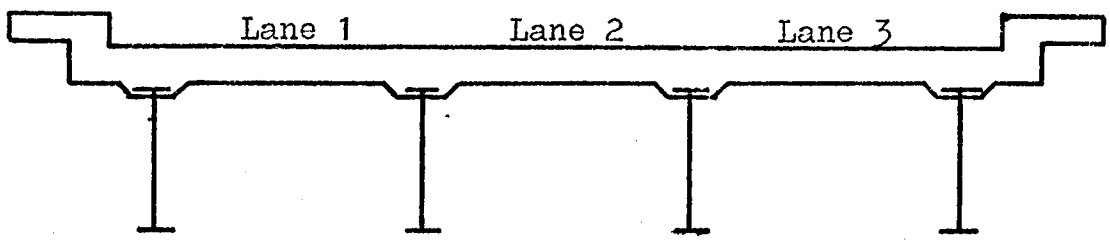


FIGURE 15. COMPARISON OF DISTRIBUTION COEFFICIENTS FOR DIFFERENT VEHICLES (OR COMBINATIONS) IN LANE 2



BRIDGE 1

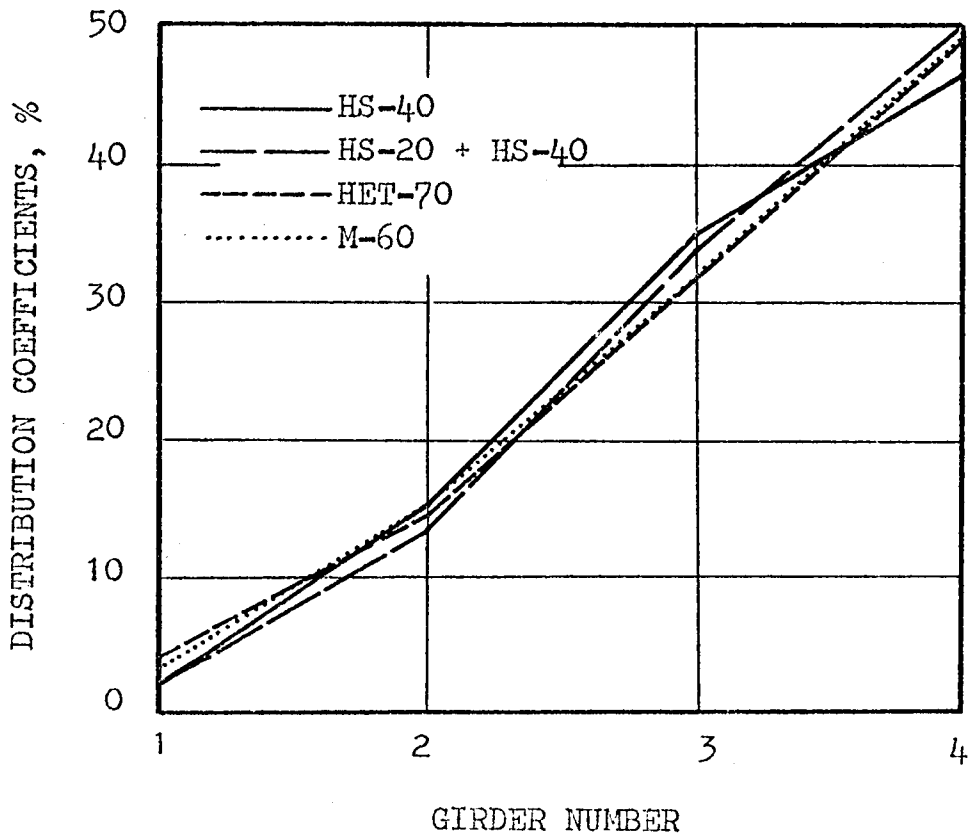


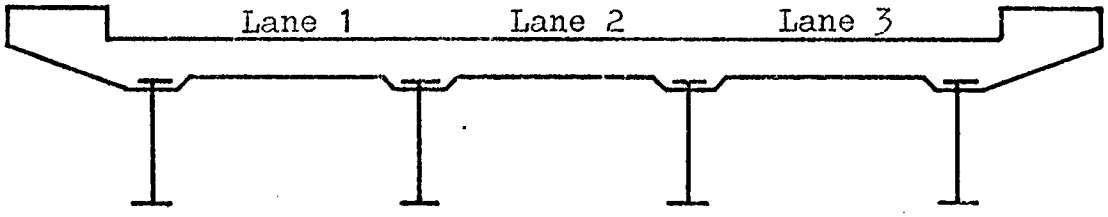
FIGURE 16. COMPARISON OF DISTRIBUTION COEFFICIENTS FOR DIFFERENT VEHICLES (OR COMBINATIONS) IN LANE 3

TABLE 5

LOAD DISTRIBUTION COEFFICIENTS - BRIDGE 4

ROLLING LOAD TESTS

Test Vehicle	Lane Number	Vehicle Speed	Direction of Travel	Distribution Coefficients, % 1	2	3	4
HS-40	1	Crawl	South	48	27	17	8
HS-40	2	Crawl	South	23	25	29	23
HS-40	3	Crawl	South	5	21	25	49
HS-40	1	10 mph	South	41	33	19	7
HS-40	2	10 mph	South	21	32	33	14
HS-40	3	10 mph	South	-	-	-	-
HS-40	1	20 mph	South	42	34	18	6
HS-40	2	20 mph	South	20	29	30	21
HS-40	3	20 mph	South	-	-	-	-
HS-40	1	Crawl	North	43	30	20	7
HS-40	2	Crawl	North	22	27	27	24
HS-40	3	Crawl	North	5	20	28	47
HS-20	1	Crawl	South	36	40	19	5
HS-20	2	Crawl	South	21	29	30	20
HS-20	3	Crawl	South	5	16	35	44



BRIDGE 4

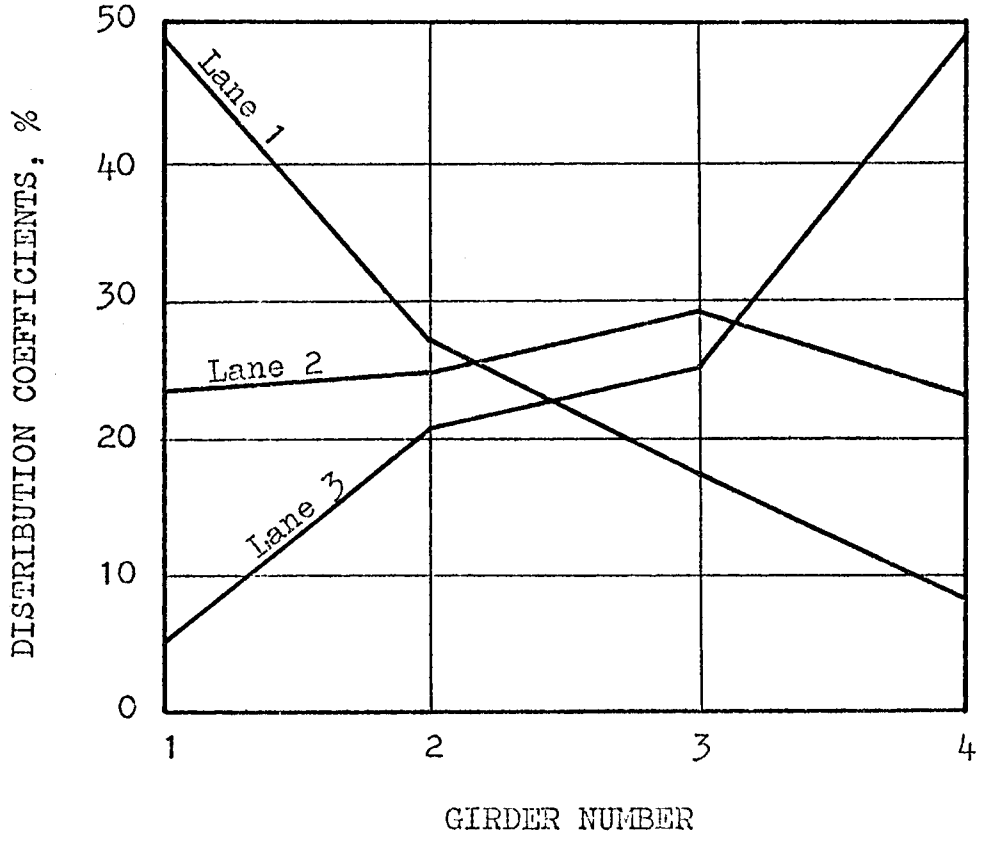
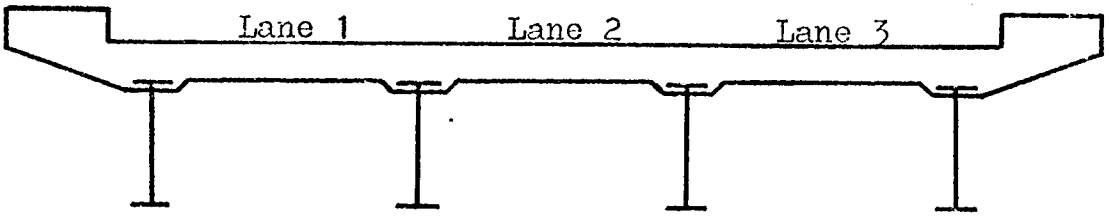


FIGURE 17. DISTRIBUTION COEFFICIENTS FOR HS-40 TRUCK IN LANES 1, 2, AND 3 TRAVELLING SOUTHBOUND



BRIDGE 4

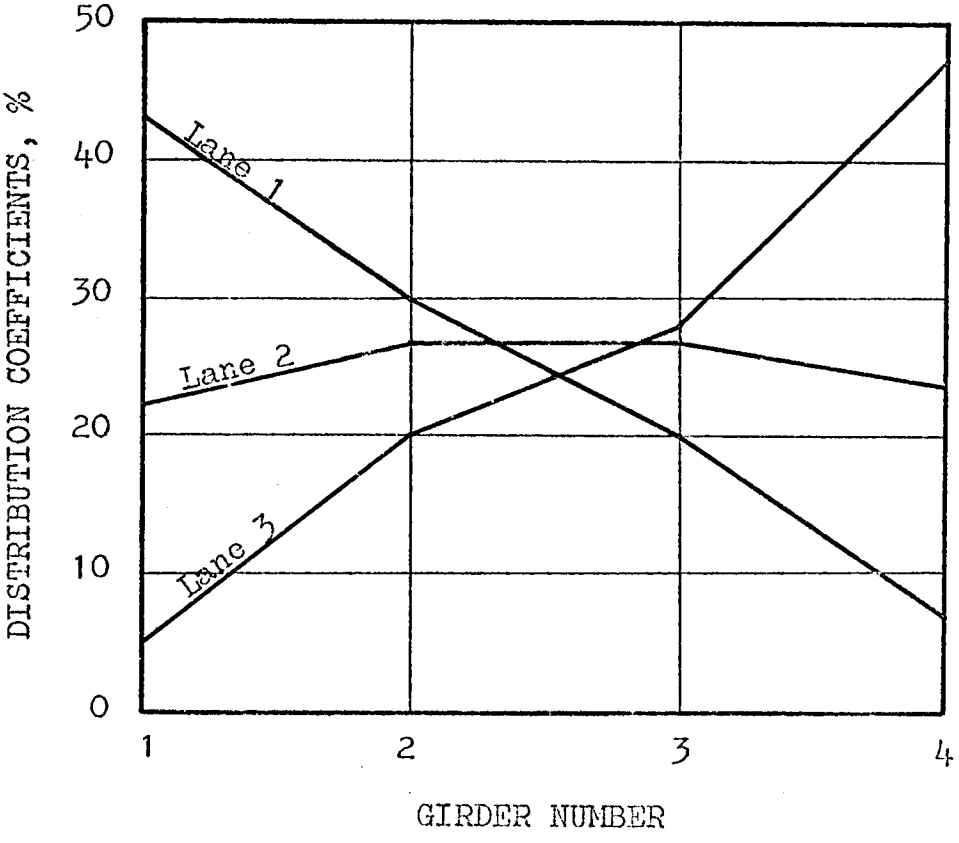
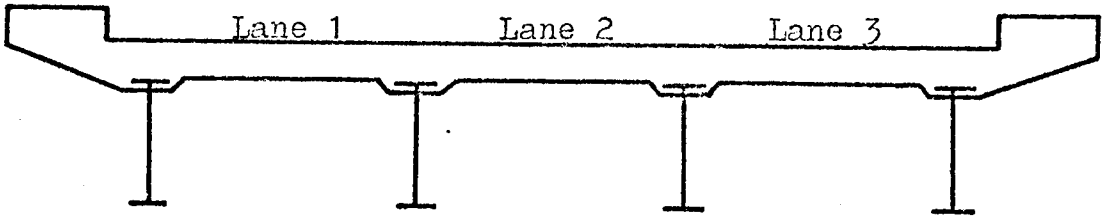


FIGURE 18. DISTRIBUTION COEFFICIENTS FOR HS-40 TRUCK IN LANES 1, 2, AND 3 TRAVELLING NORTHBOUND



BRIDGE 4

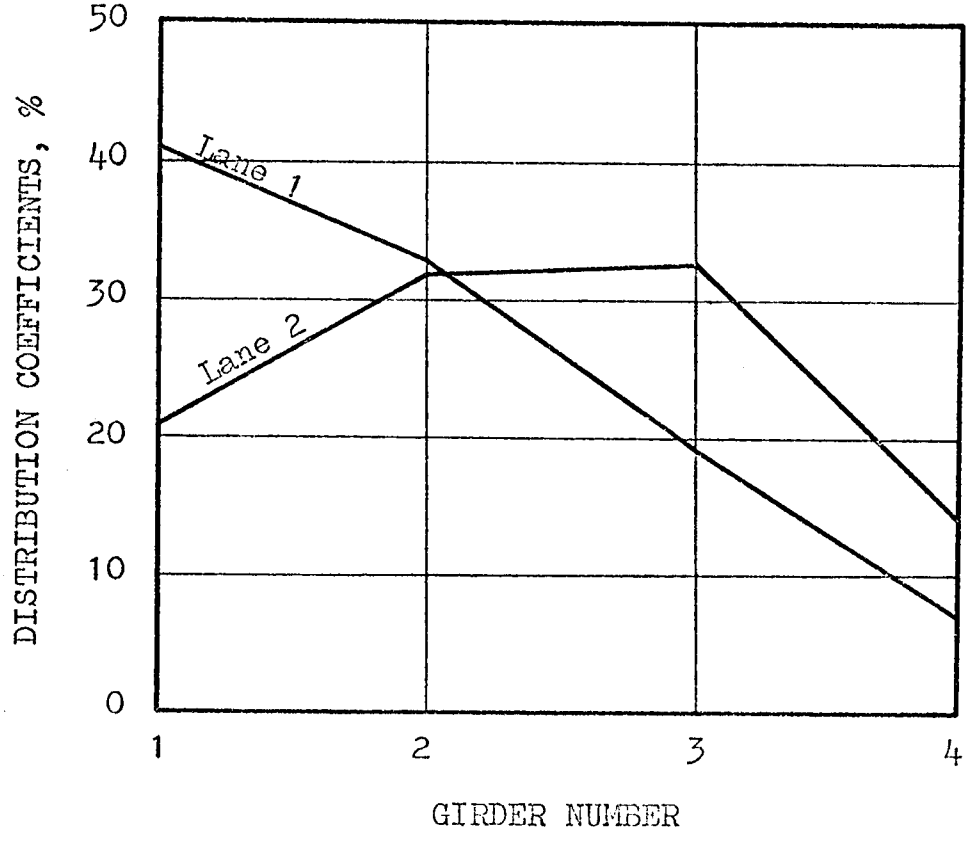
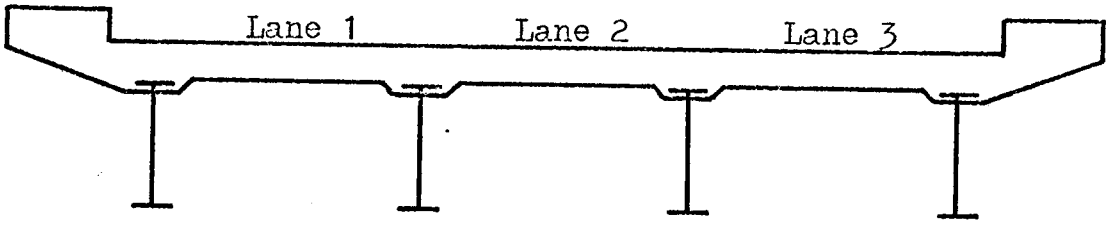


FIGURE 19. DISTRIBUTION COEFFICIENTS FOR HS-40 TRUCK IN LANES 1 AND 2 TRAVELLING AT 10 MPH



BRIDGE 4

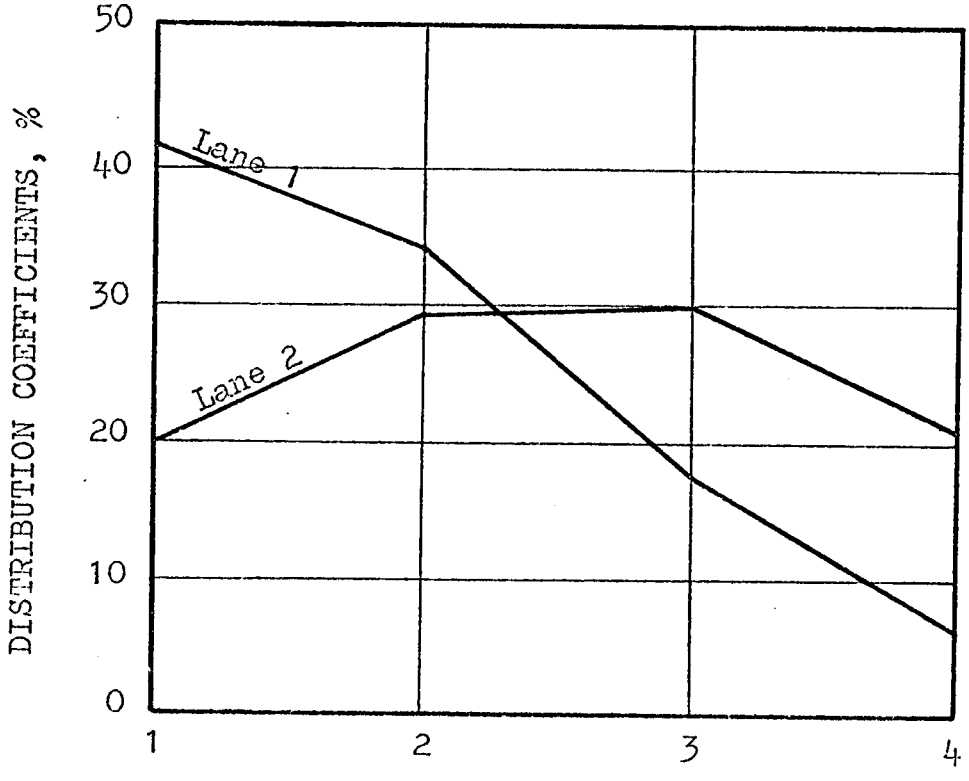
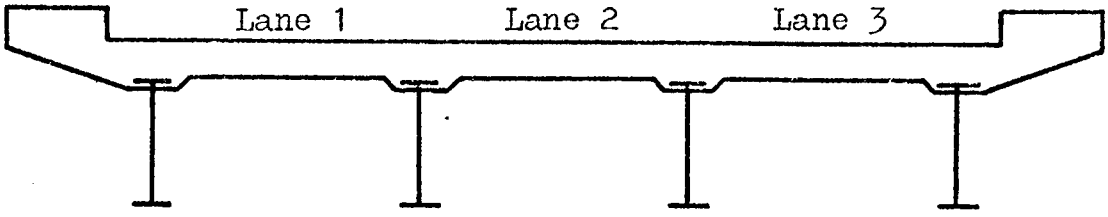


FIGURE 20. DISTRIBUTION COEFFICIENTS FOR HS-40 TRUCK IN LANES 1 AND 2 TRAVELLING AT 20 MPH



BRIDGE 4

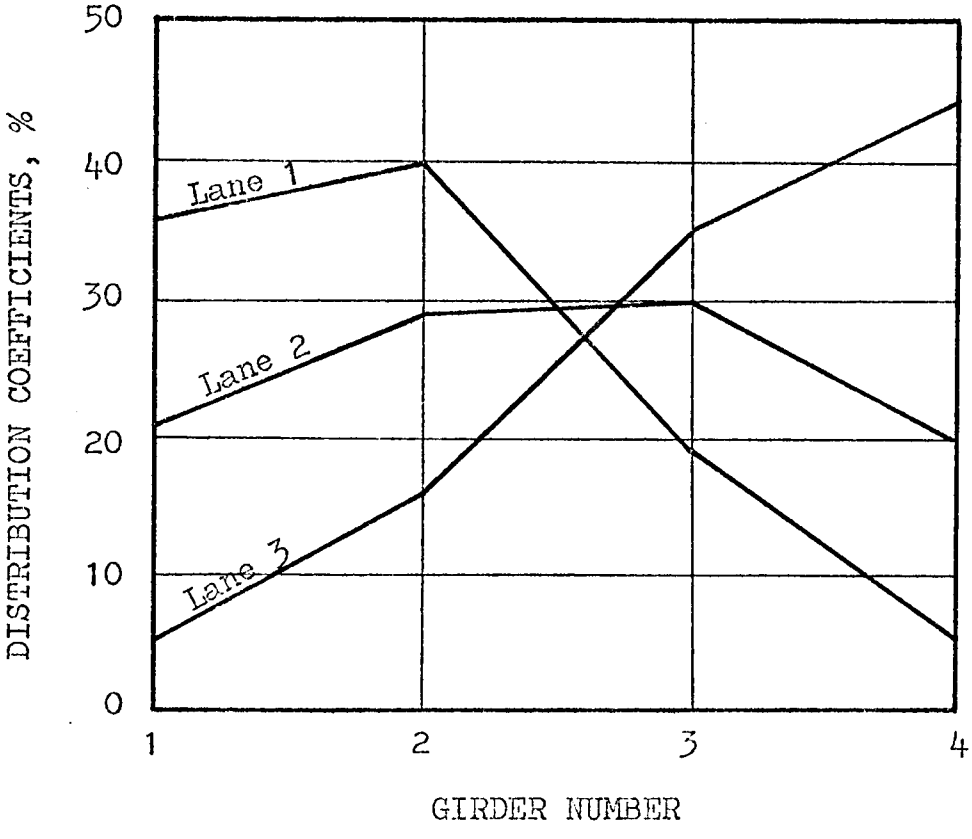
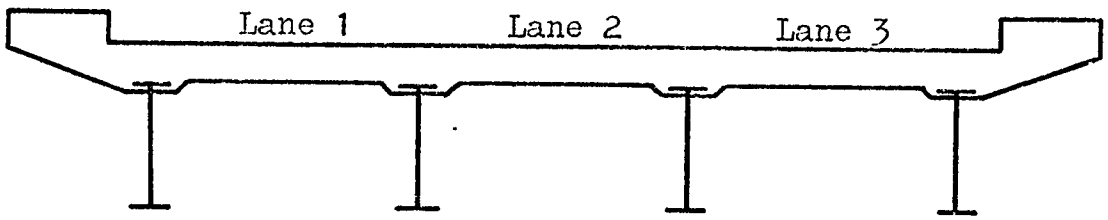


FIGURE 21. DISTRIBUTION COEFFICIENTS FOR HS-20 TRUCK IN LANES 1, 2, AND 3



BRIDGE 4

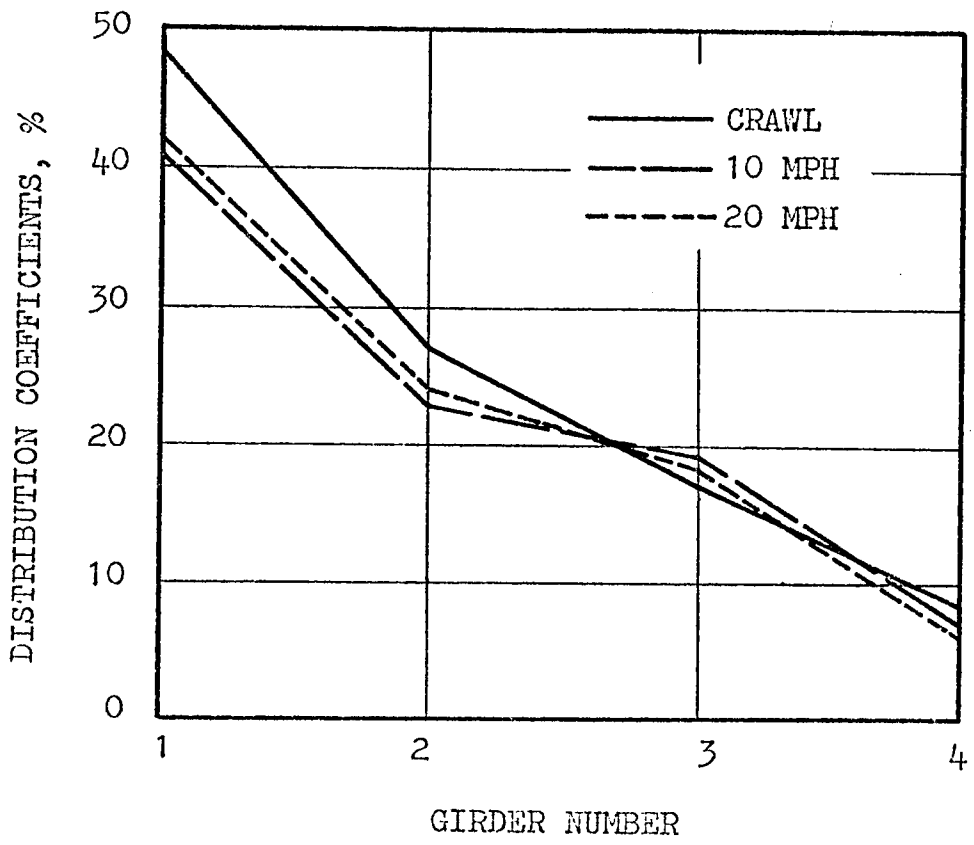
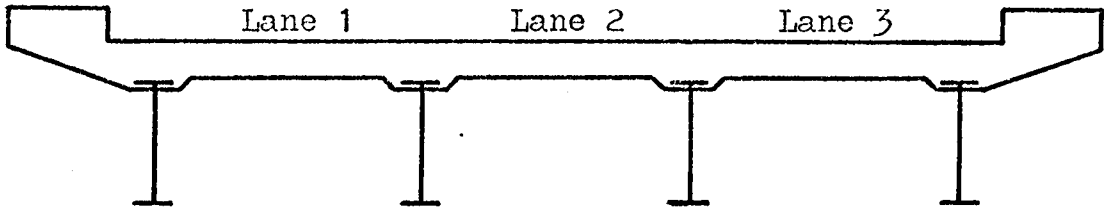


FIGURE 22. COMPARISON OF DISTRIBUTION COEFFICIENTS FOR HS-40 TRUCK IN LANE 1 TRAVELLING AT CRAWL SPEED, 10 MPH, AND 20 MPH



BRIDGE 4

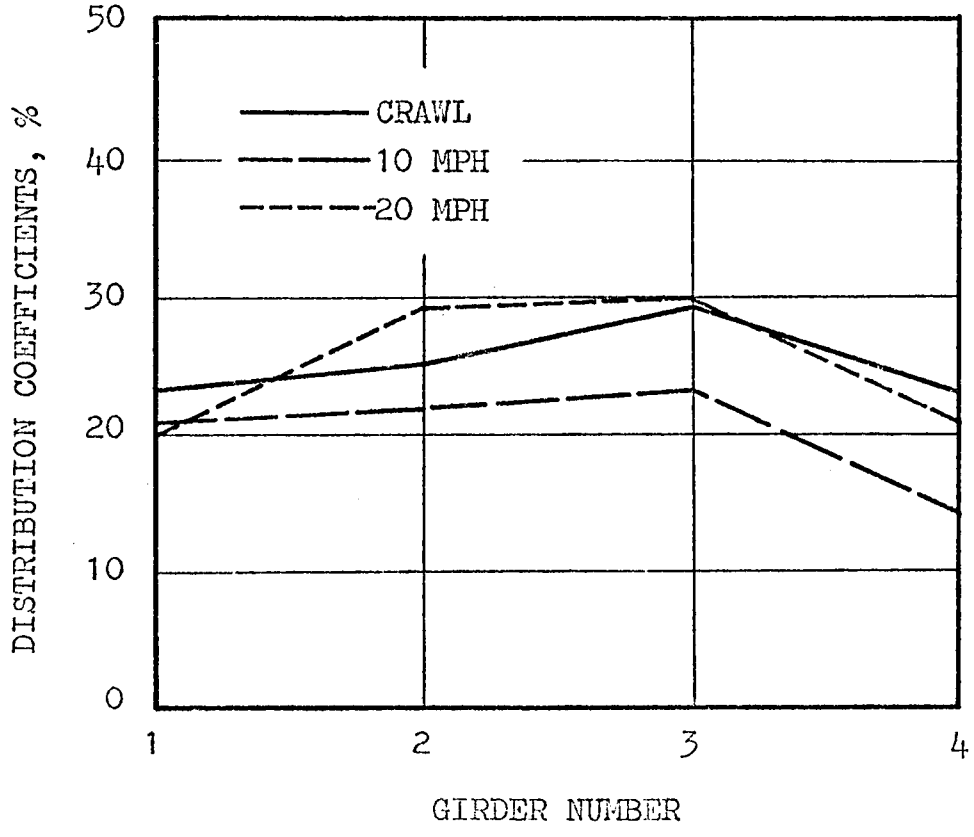
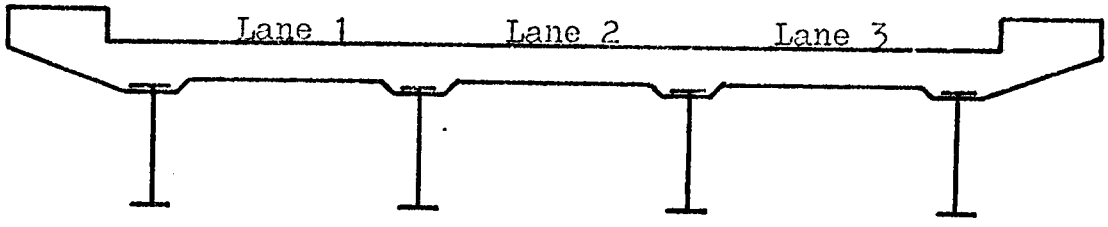


FIGURE 23. COMPARISON OF DISTRIBUTION COEFFICIENTS FOR HS-40 TRUCK IN LANE 2 TRAVELLING AT CRAWL SPEED, 10 MPH, AND 20 MPH



BRIDGE 4

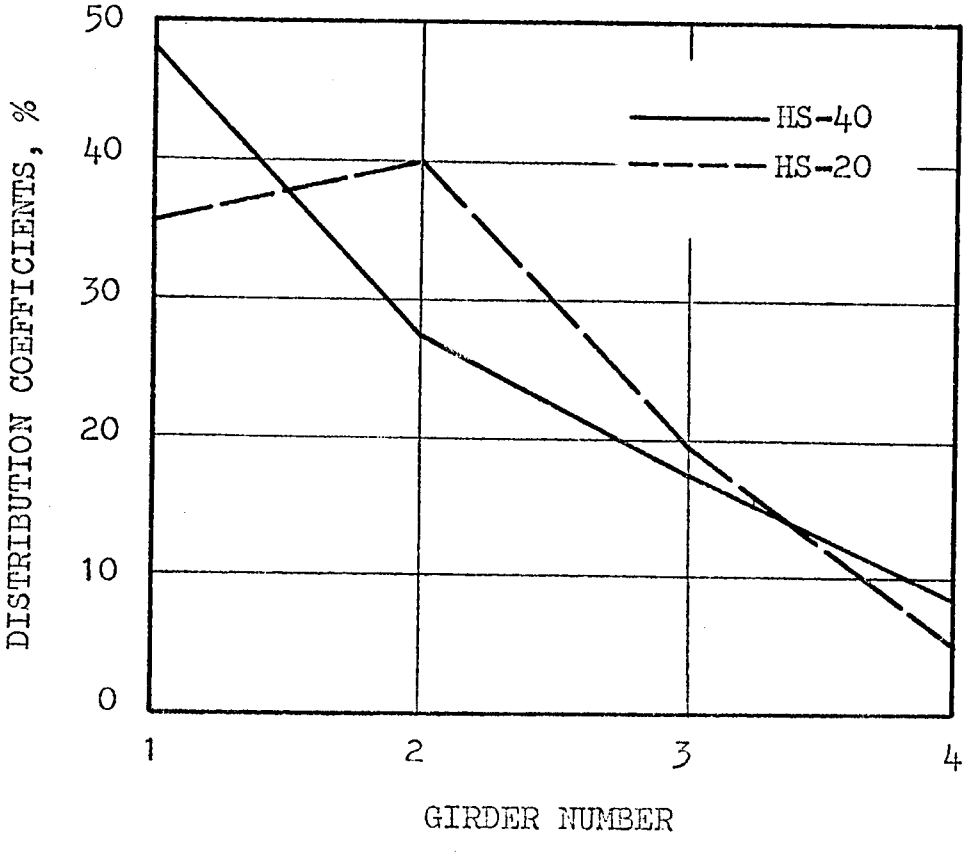
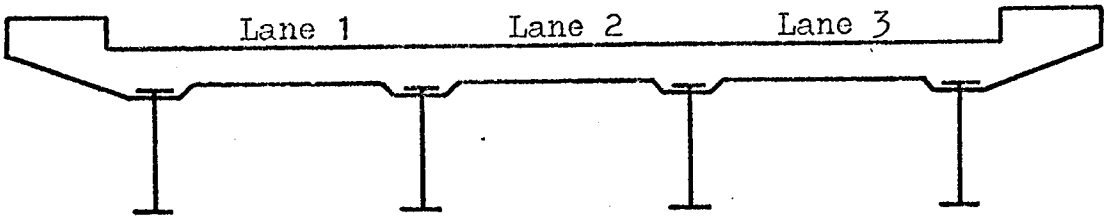


FIGURE 24. COMPARISON OF DISTRIBUTION COEFFICIENTS FOR HS-40 AND HS-20 TRUCKS IN LANE 1



BRIDGE 4

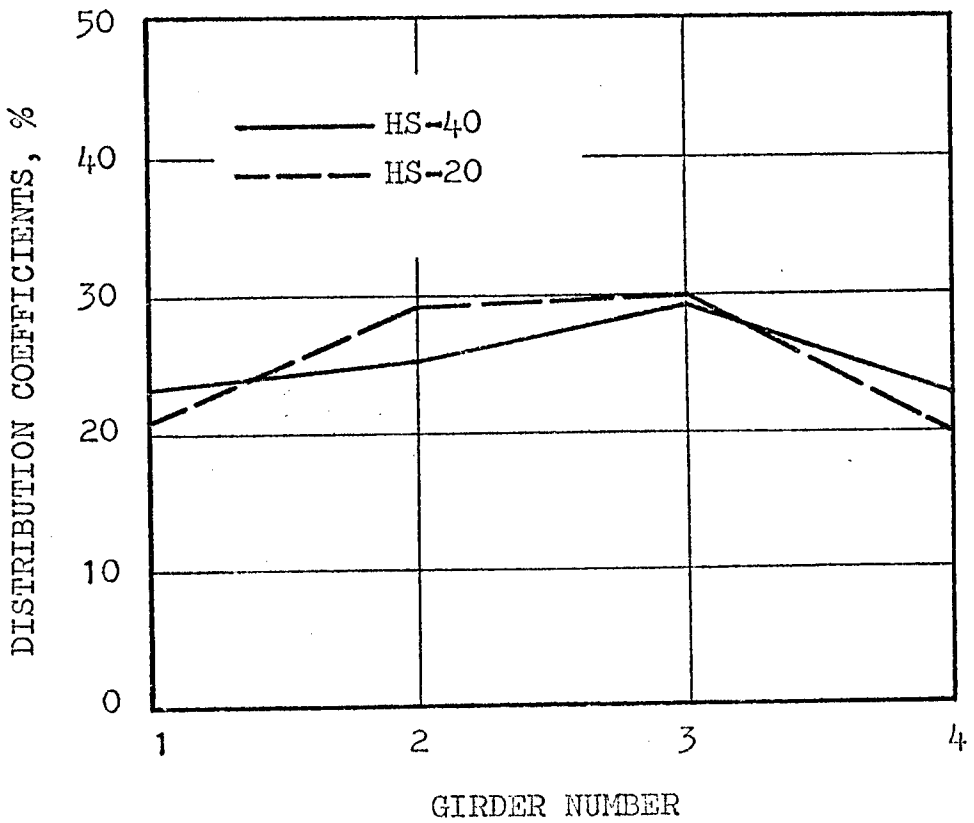
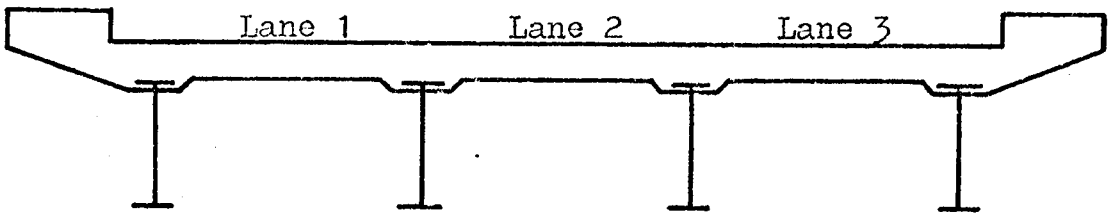


FIGURE 25. COMPARISON OF DISTRIBUTION COEFFICIENTS FOR HS-40 AND HS-20 TRUCKS IN LANE 2



BRIDGE 4

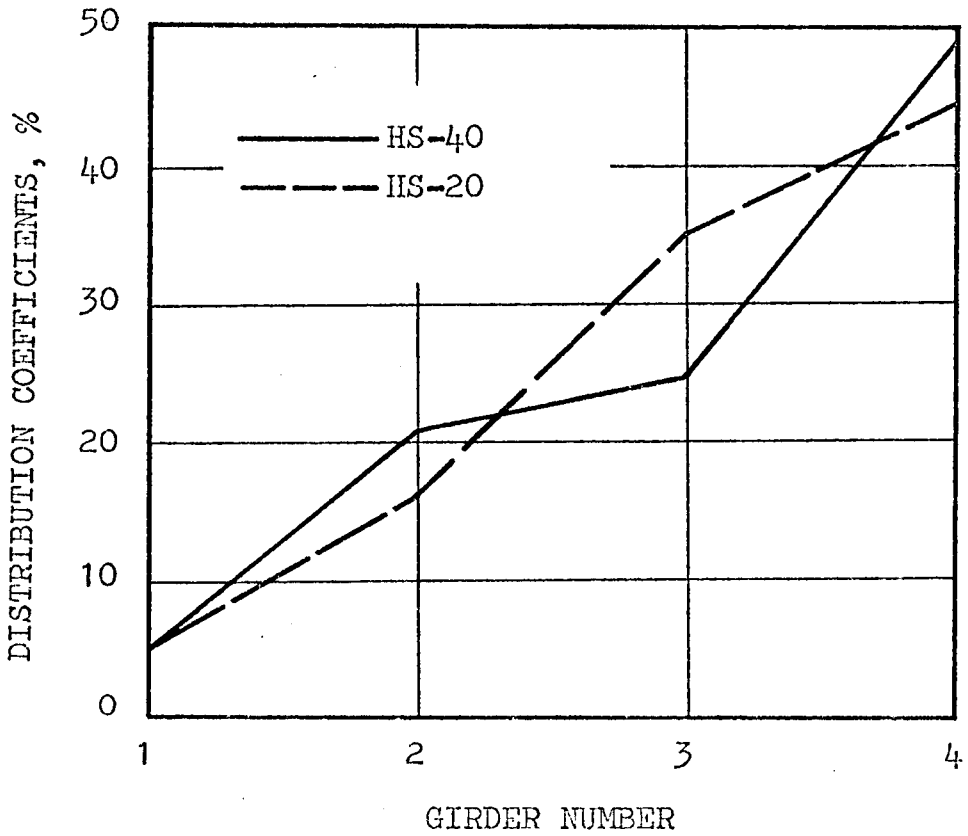


FIGURE 26. COMPARISON OF DISTRIBUTION COEFFICIENTS FOR HS-40 AND HS-20 TRUCKS IN LANE 3

TABLE 6

LOAD DISTRIBUTION COEFFICIENTS - BRIDGE 1
STATIC LOAD TESTS TO FAILURE

Load at Each Point	Total Load on Bridge	Distribution Coefficients, % 1	2	3	4
12 kip	96 kip	18	29	30	23
32 kip	256 kip	20	29	29	22
54 kip	432 kip	20	26	29	25
67 kip	536 kip	20	27	29	24
81 kip	648 kip	20	27	30	23
87 kip	696 kip	20	28	30	22
99 kip	792 kip	21	29	30	20

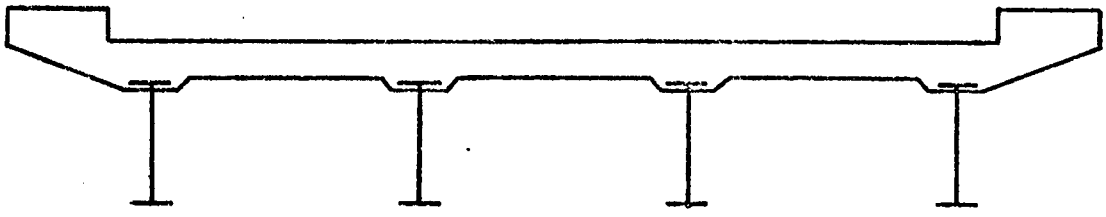
due to equal forces applied at each of the eight points shown in Figure 7 (p. 18).

Static Load Tests - Bridge 4. The coefficients in Table 7 indicate the lateral distribution of load on Bridge 4 due to forces at various combinations of the six points shown in Figure 8 (p. 19). The distribution coefficients for two different loading patterns are shown in Figures 27 and 28.

TABLE 7

LOAD DISTRIBUTION COEFFICIENTS - BRIDGE 4
STATIC LOAD TESTS TO FAILURE

Load Location	Load at Each Point	Total Load on Bridge	Distribution Coefficients, % 1	2	3	4
A,B	28 kip	56 kip	38	34	22	6
A,B	59 kip	118 kip	37	34	22	7
A,B,C,D	28 kip	112 kip	22	28	29	21
A,B,C,D	59 kip	236 kip	22	28	29	21
C,D,E,F	28 kip	112 kip	7	20	34	29
C,D,E,F	59 kip	236 kip	7	21	36	36
A	59 kip	59 kip	54	33	13	0
B	59 kip	59 kip	23	39	33	5
C	59 kip	59 kip	12	32	45	11
D	59 kip	59 kip	1	11	32	56
All	16 kip	96 kip	20	28	24	28
All	28 kip	168 kip	19	29	26	26
All	38 kip	228 kip	20	28	26	26
All	49 kip	294 kip	20	28	26	26
All	59 kip	354 kip	21	28	25	26



BRIDGE 4

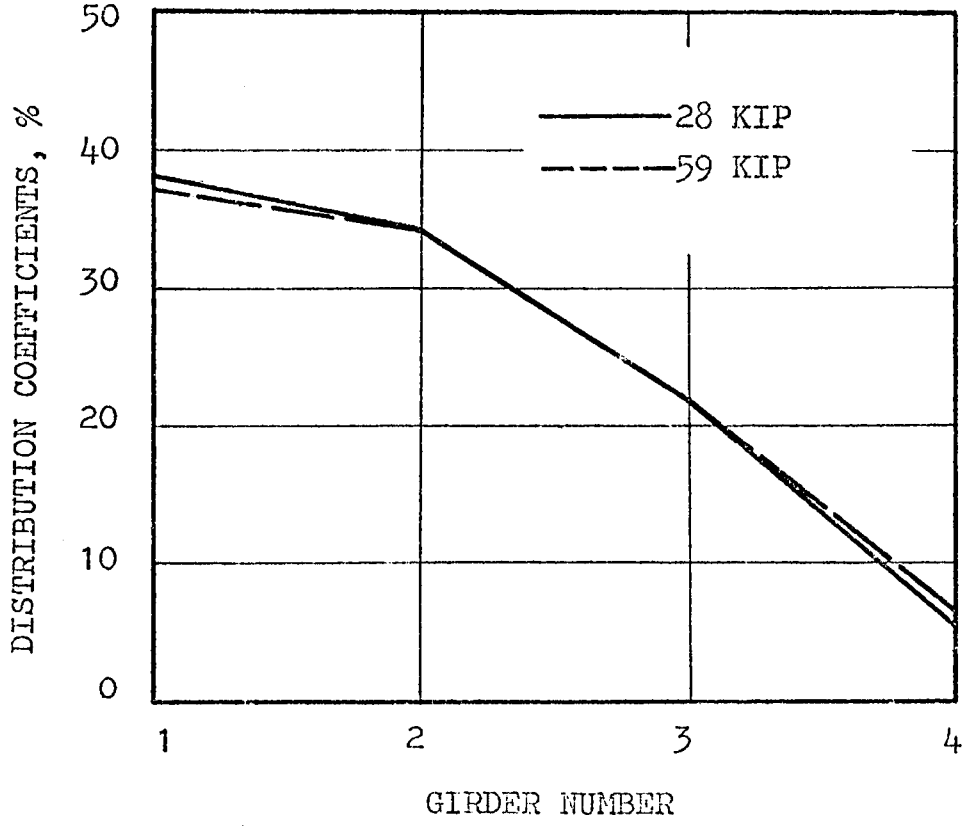
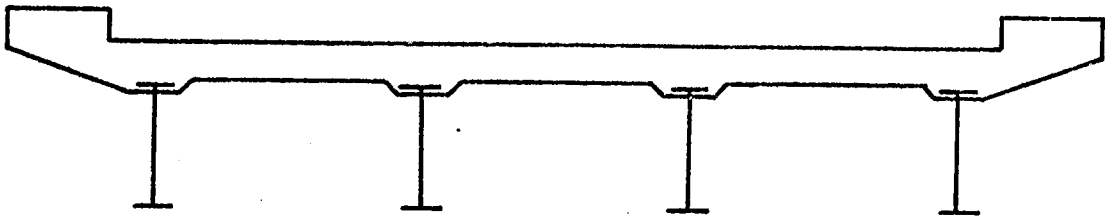


FIGURE 27. DISTRIBUTION COEFFICIENTS FOR STATIC TESTS TO FAILURE WITH LOADS AT POINTS A AND B ONLY



BRIDGE 4

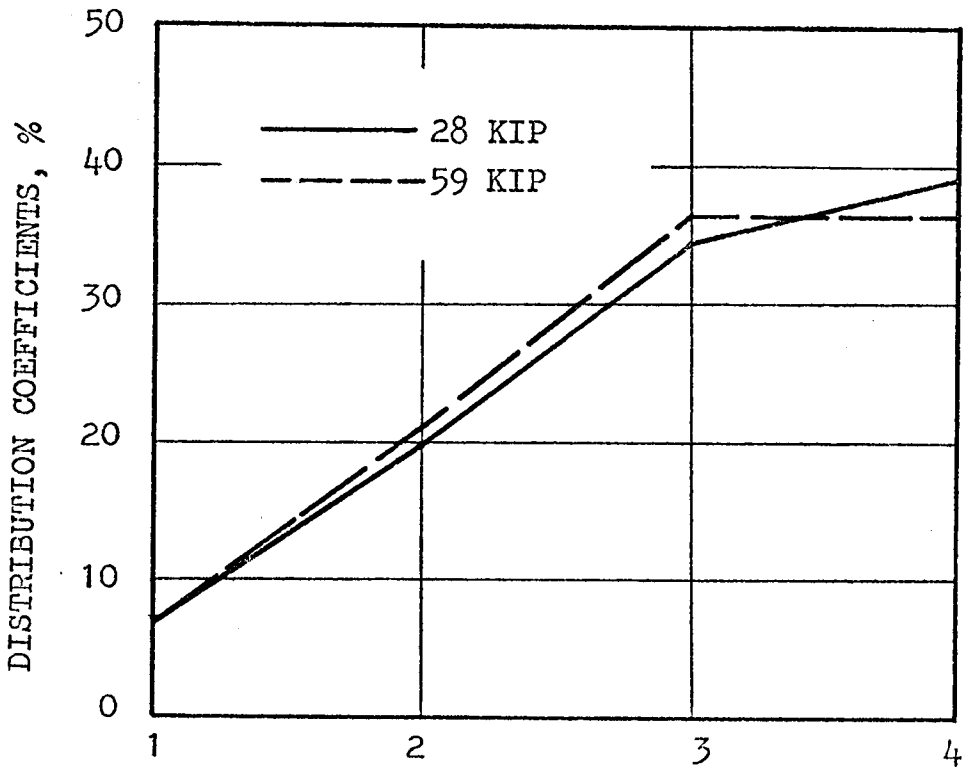


FIGURE 28. DISTRIBUTION COEFFICIENTS FOR STATIC TESTS TO FAILURE WITH LOADS AT POINTS C, D, E, AND F

CHAPTER V

PREDICTION OF LATERAL DISTRIBUTION

The theoretical analysis of bridges to determine the lateral distribution of load is a difficult, time-consuming, and therefore expensive process. For over thirty years AASHO has published and authorized the use of an empirical method of distribution to simplify the problem. Since that time numerous researchers have advanced their own theories and proposed revisions to the AASHO load distribution equation. This chapter will compare the results of the full scale bridge tests reported herein to the current AASHTO specifications, the proposed revisions of Sanders and Elleby, the proposed changes of Motarjemi and Van Horn, and a STRUDL analysis of each bridge.

Explanation of Distribution Methods

AASHTO Specifications. The current AASHTO Specifications (5) state for a two lane bridge with a concrete deck over I-beam stringers spaced not more than fourteen feet apart that the live load bending moment for each interior stringer shall be determined by applying the fraction S/5.5 (S= stringer spacing) of a wheel load (both front and rear) to the stringer. For a similar bridge the live laod bending moment for an exterior stringer is determined by applying the fraction S/(4.0+0.25S) of a wheel load to the stringer.

Sanders and Elleby Proposal. In their final report, Sanders and Elleby (6) recommend significant changes to the AASHTO Specifications for determining lateral distribution of load. Specifically, they recommend for beam and slab bridges that the live load bending moment for each beam (interior and exterior) be determined by applying the fraction of a wheel load (both front and rear) determined by the following:

$$\text{Load Fraction} = \frac{S}{D}$$

where,

$$D = 5 + \frac{NL}{10} + (3 - \frac{2NL}{7})(1 - \frac{C}{3})^2, \text{ when } C \leqslant 3$$

$$D = 5 + \frac{NL}{10}, \text{ when } C > 3$$

where,

S = average beam spacing, ft.

NL = total number of design traffic lanes

C = a stiffness parameter which depends upon the type of bridge, bridge and beam geometry, and material properties

For steel beam and concrete slab bridges, the value of C is to be calculated using the relationship:

$$C = \frac{W}{L} \left(\frac{E}{2G} \times \frac{I1}{J1 + Jt}\right)^{\frac{1}{2}}$$

where,

W = overall width of the bridge, ft.

L = span length, ft. (distance between points of inflection for continuous spans)

E = modulus of elasticity of the transformed beam section

G = modulus of rigidity of the transformed beam section

I1 = flexural moment of inertia of the transformed beam section per unit width

J1 = torsional moment of inertia of the transformed beam section per unit width

Jt = one half of the torsional moment of inertia of a unit width of the slab

or for preliminary calculations C may be expressed as:

$$C = K \times \frac{W}{L}$$

where,

K = 3.0 for non-composite steel I-beams

K = 4.8 for composite steel I-beams

Motarjemi and Van Horn Recommendations. In their report on prestressed concrete box-beam bridges (7), Motarjemi and Van Horn recommend a new procedure for determination of the lateral distribution factors for spread box beam bridges. While their research was stated to be limited to concrete box-beams only, their procedure will be used directly to compute distribution factors for the steel beam bridges of this report for comparison purposes. Their procedure was developed by theoretical analysis of the various parameters involved. Based on this analysis and the results of earlier tests (8, 9, 10, 11, 12, 13, 14) , they recommend the following formula for determining distribution factors for interior beams:

$$D.F. = \frac{2NL}{NB} + k\frac{S}{L}$$

where,

$$k = 0.07W - NL(0.10NL - 0.26) - 0.20NB - 0.12$$

W = roadway width between curbs, ft.

NL = number of design traffic lanes

NB = number of beams

S = average beam spacing

L = span length

They further recommend the live load bending moments for exterior girders be determined by applying the reaction of wheel loads by assuming the flooring to act as a simple span between the exterior and adjacent interior beams, but not less than 2NL/NB.

STRUDL II Analyses. Both bridges were modeled using the STRUDL II subset of the ICES computer program. The models included a combination of plate bending elements to simulate the concrete deck and grid members to simulate the longitudinal beams.

Bogaty (3) divided the concrete deck of Bridge 1 into 256 finite elements including stiffer elements along the edges of the roadway to simulate the curbs. The effect of the handrails was neglected. The longitudinal beams were divided into ten ft. long grid elements. The additional stiffness at cover plated sections was included and, for the results used in this comparison, the girder section properties were programmed to align the top of the girder with the bottom of the slab in order to closely simulate composite action. The HS-40 loading was applied to the model at the longitudinal position yielding maximum moment. The lateral position

was varied in two foot increments, and these data were used to construct the distribution coefficient influence lines shown in Figure 29. Distribution factors for interior and exterior girders are determined by superimposing the influence line values for two trucks in the desired position.

Rush (4) divided the concrete deck of Bridge 4 into one hundred sixty finite elements including stiffer curb elements. The longitudinal beams were divided into 7.5 ft. long grid elements including the effects of coverplates. The analysis was made with the centroid of the grid elements (beams) aligned with the centroid of the plate elements (slab). The HS-40 loading was applied to the model to produce maximum positive moment in the center span. The lateral position was varied in two foot increments, and these data were used to construct the distribution coefficient influence lines shown in Figure 30. Distribution factors for interior and exterior girders are determined by superimposing the influence line values for two trucks in the desired position.

Since the distribution coefficient represents the load related to the entire truck and the distribution factor represents the load related to one line of wheels, the distribution factor is obtained by doubling the sum of the two superimposed distribution coefficients.

Rolling Load Test Results. Rolling load tests were performed in three test lanes on each bridge. As shown in Figure 2 (p. 6) and Figure 3 (p. 7), these test lanes were

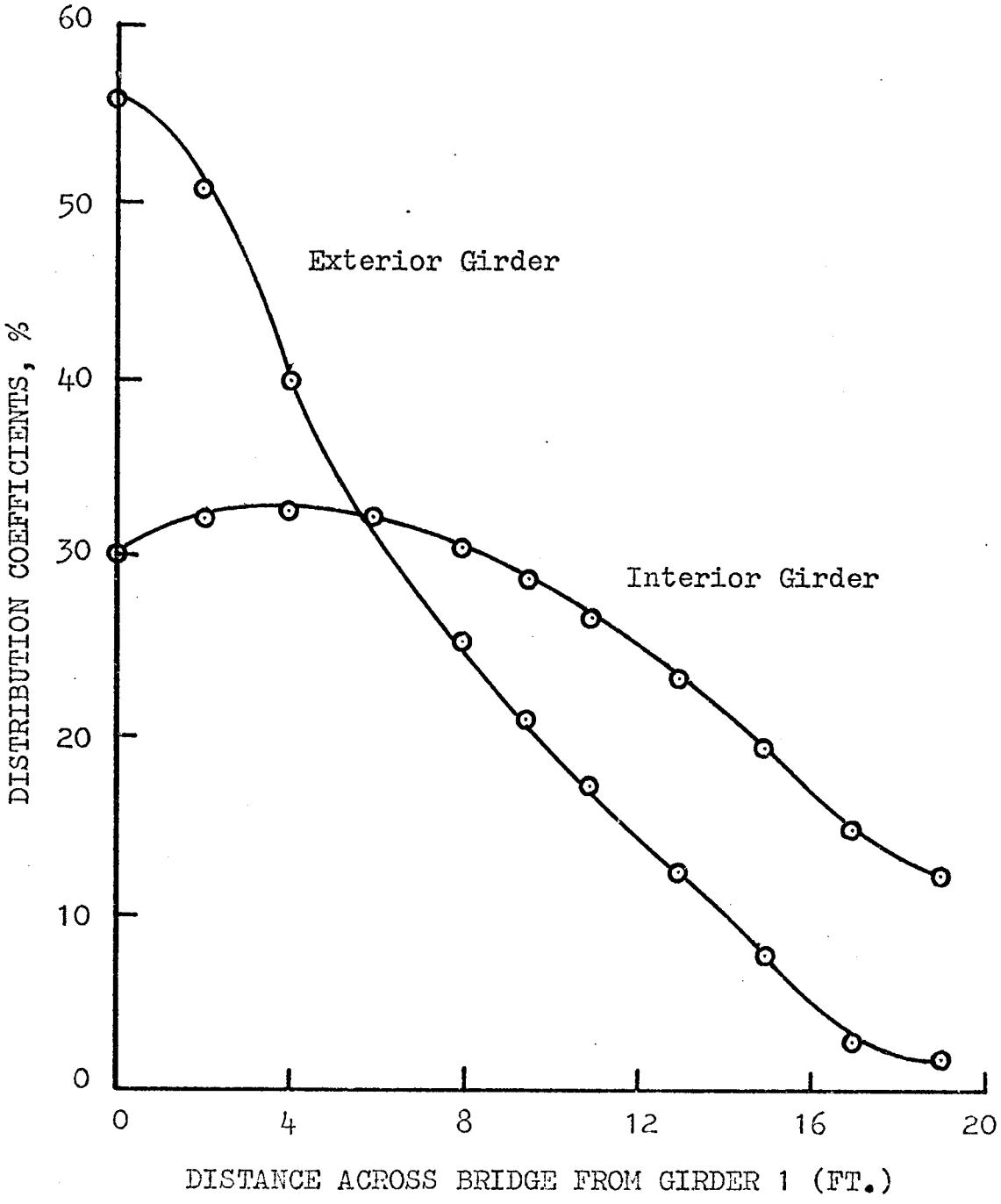


FIGURE 29. LOAD DISTRIBUTION COEFFICIENT INFLUENCE LINES FOR A SINGLE HS-40 VEHICLE ON BRIDGE 1 (3, p. 20)

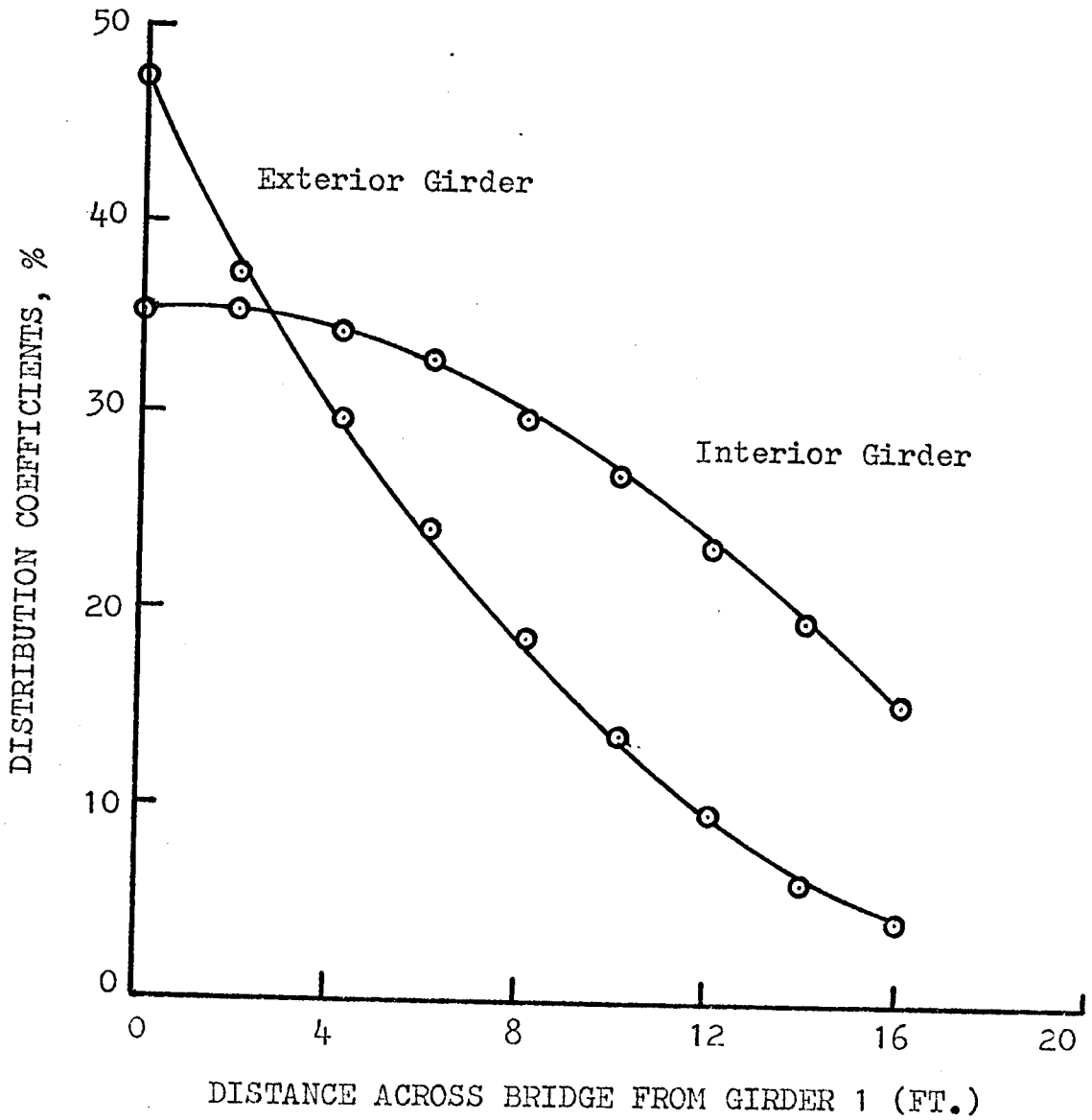


FIGURE 30. LOAD DISTRIBUTION COEFFICIENT INFLUENCE LINES FOR A SINGLE HS-40 VEHICLE ON BRIDGE 4 (4, p. 13)

located between girders. Distribution factors are computed by superimposing the distribution coefficients of a given girder for two tests. Distribution factors are first computed with vehicles in test lanes 1 and 3 to simulate the actual service conditions of the bridge. Distribution factors are then computed with vehicles in test lanes 1 and 2 to obtain the maximum possible factors to compare with the recommended AASHTO values. The actual placement of two eight foot wide trucks side by side in Lanes 1 and 2 on Bridge 4 is not exactly possible since the test lanes were only 7'-4" wide. For the purposes of comparison, this superposition will be made herein since there is only an eight inch discrepancy.

Distribution Factors - Bridge 1

AASHTO Specifications.

$$\text{Interior Girder D. F.} = \frac{S}{5.5} = \frac{8.33}{5.5} = 1.51$$

$$\text{Exterior Girder D. F.} = \frac{S}{4.0 + 0.25S} = \frac{8.33}{6.08} = 1.36$$

Sanders and Elleby Proposal. For preliminary designs the stiffness parameter is calculated as:

$$C = K \times \frac{W}{L} = 4.8 \times \frac{28.0}{67.5} = 1.99$$

and for final designs C is calculated as previously defined. As stated in Appendix B of Sanders and Elleby, for composite steel and concrete, this relationship reduced to the following with Poisson's ratio = 0.2.

$$C = 3.0 \frac{W}{L} \left(\frac{nIb}{St^3}\right)^{\frac{1}{2}}$$

$$= 4.98 \times \frac{28.0}{67.5}$$

$$= 2.06$$

where,

n = modular ratio Es/Ec

S = beam spacing

t = slab thickness

Using the final design value for the stiffness parameter (C = 2.06), the distribution factor is computed.

$$D = 5 + \frac{2}{10} + (3 - \frac{4}{7})(1 - \frac{2.06}{3})^2$$

$$= 5.74$$

$$\text{Distribution Factor} = \frac{S}{D}$$

$$= \frac{8.33}{5.74}$$

$$= 1.45$$

Motarjemi and Van Horn Recommendations. For Bridge 1 the parameter k is evaluated as

$$k = 0.07W - NL(0.10NL - 0.26) - 0.20NB - 0.12$$

$$= 1.96 - 2(0.20 - 0.26) - 0.80 - 0.12$$

$$= 1.16$$

The interior girder distribution factor may now be computed.

$$\text{Interior Girder D. F.} = \frac{4}{4} + 1.16 \times \frac{8.33}{67.5}$$

$$= 1.14$$

With the outside wheels directly over an exterior girder and the deck acting as a simple span, the resulting exterior distribution factor may now be computed.

$$\text{Exterior Girder D. F.} = 1.0 + \frac{2.33}{8.33}$$

$$= 1.28$$

STRUDL II Analysis. Distribution factors are first computed by combining distribution coefficients for a truck in Lane 1 and a second truck in Lane 3.

$$\text{Interior Girder D. F.} = 2\ (0.31 + 0.15)$$

$$= 0.92$$

$$\text{Exterior Girder D. F.} = 2\ (0.55 + 0.03)$$

$$= 1.16$$

The maximum distribution factors as used in design are obtained by combining distribution coefficients for a truck in Lane 1 and a second truck in Lane 2.

$$\text{Interior Girder D. F.} = 2\ (0.31 + 0.29)$$

$$= 1.20$$

$$\text{Exterior Girder D. F.} = 2\ (0.55 + 0.23)$$

$$= 1.56$$

Rolling Load Test Results. Distribution factors are first computed by combining the load distribution coefficients from Table 4 (p. 26) for a given vehicle in Lane 1 and the same vehicle in Lane 3. For the purpose of comparison,

distribution factors are computed with four different vehicles.

Interior Girder D. F.

HS-40 = 1.08

HS-20 + HS-40 = 1.02

M-60 = 0.96

HET-70 = 0.94

Exterior Girder D. F.

HS-40 = 0.96

HS-20 + HS-40 = 1.06

M-60 = 1.04

HET-70 = 1.06

The following distribution factors are computed with a given vehicle in test Lane 1 and the same vehicle in test Lane 2.

Interior Girder D. F.

HS-40 = 1.38

HS-20 + HS-40 = 1.26

Exterior Girder D. F.

HS-40 = 1.32

HS-20 + HS-40 = 1.40

All of the computed distribution factors for Bridge 1 are shown in Table 8. Since the load distribution equation D.F. = S/D is a very familiar one, the term "D" is also tabulated for comparison.

TABLE 8

COMPARISON OF DISTRIBUTION FACTORS
FOR BRIDGE 1

Method	Interior Girder D.F.	Interior Girder "D"	Exterior Girder D.F.	Exterior Girder "D"
AASHTO Specifications	1.51	5.50	1.36	6.08
Sanders and Elleby	1.45	5.74	1.45	5.74
Motarjemi and Van Horn	1.14	7.31	1.28	6.51
STRUDL with Vehicle in Lanes 1 and 3	0.92	9.06	1.16	7.17
STRUDL with Vehicle in Lanes 1 and 2	1.20	6.94	1.56	5.35
HS-40 Test Vehicle in Lanes 1 and 3	1.08	7.71	0.96	8.68
HS-40 Test Vehicle in Lanes 1 and 2	1.38	6.04	1.32	6.30
HS-20 and HS-40 Test Vehicles in Lanes 1 and 3	1.02	8.16	1.06	7.85
HS-20 and HS-40 Test Vehicles in Lanes 1 and 2	1.26	6.60	1.40	5.95
M-60 Tank in Lanes 1 and 2	0.96	8.68	1.04	8.00
HET-70 Truck in Lanes 1 and 2	0.94	8.86	1.06	7.85

Distribution Factors - Bridge 4

AASHTO Specifications.

$$\text{Interior Girder D. F.} = \frac{7.33}{5.5}$$

$$= 1.33$$

$$\text{Exterior Girder D. F.} = \frac{7.33}{5.83}$$

$$= 1.26$$

Sanders and Elleby Proposal. The preliminary stiffness parameter is calculated as:

$$C = 3.0 \times \frac{23.0}{45.0}$$

$$= 1.53$$

and for final designs the stiffness parameter is calculated as:

$$C = 1.97 \times \frac{23.0}{45.0}$$

$$= 1.01$$

Using the final design value for the stiffness parameter (C = 1.01), the distribution factors are now computed.

$$D = 5 + \frac{2}{10} + (3 - \frac{4}{7})(1 - \frac{1.01}{3})^2$$

$$= 5.84$$

$$\text{Distribution Factor} = \frac{7.33}{5.84}$$

$$= 1.25$$

Motarjemi and Van Horn Recommendations. For Bridge 4 the parameter k is evaluated as:

$$k = 1.61 - 2\,(0.20 - 0.26) - 0.8 - 0.12$$

$$= 0.81$$

The interior girder distribution factor may now be computed.

$$\text{Interior Girder D. F.} = \frac{4}{4} + 0.81 \times \frac{7.33}{45.0}$$

$$= 1.13$$

With the outside wheels directly over an exterior girder and the deck acting as a simple span, the resulting exterior distribution factor may now be computed.

$$\text{Exterior Girder D. F.} = 1.0 + \frac{1.33}{7.33}$$

$$= 1.18$$

STRUDL II Analysis. Distribution factors are first computed by combining distribution coefficients for a truck in Lane 1 and a second truck in Lane 3.

$$\text{Interior Girder D. F.} = 2\ (0.35 + 0.17)$$

$$= 1.04$$

$$\text{Exterior Girder D. F.} = 2\ (0.47 + 0.05)$$

$$= 1.04$$

The maximum distribution factors as used in design are obtained by combining distribution coefficients for a truck in Lane 1 and a second truck in Lane 2.

$$\text{Interior Girder D. F.} = 2\ (0.35 + 0.32)$$

$$= 1.34$$

$$\text{Exterior Girder D. F.} = 2\ (0.47 + 0.20)$$

$$= 1.34$$

Rolling Load Test Results. Distribution factors are first computed by combining the load distribution coefficients from Table 5 (p. 34) for a given vehicle in Lane 1 and the same vehicle in Lane 3. For the purpose of comparison,

distribution factors are computed for three different vehicles.

Interior Girder D. F.

HS-40 (Southbound) = 0.96

HS-40 (Northbound) = 1.00

HS-20 (Southbound) = 1.12

Exterior Girder D. F.

HS-40 (Southbound) = 1.06

HS-40 (Northbound) = 0.96

HS-20 (Southbound) = 0.82

The following distribution factors are computed with a given vehicle in test Lane 1 and the same vehicle in test Lane 2.

Interior Girder D. F.

HS-40 (Southbound) = 1.04

HS-40 (Northbound) = 1.14

HS-20 (Southbound) = 1.30

Exterior Girder D. F.

HS-40 (Southbound) = 1.44

HS-40 (Northbound) = 1.42

HS-20 (Southbound) = 1.28

All of the computed distribution factors for Bridge 4 are shown in Table 9. Since the load distribution equation D.F. = S/D is a very familiar one, the term "D" is also tabulated for comparison.

TABLE 9

COMPARISON OF DISTRIBUTION FACTORS
FOR BRIDGE 4

Method	Interior Girder D.F.	Interior Girder "D"	Exterior Girder D.F.	Exterior Girder "D"
AASHTO Specifications	1.33	5.50	1.26	5.83
Sanders and Elleby	1.25	5.84	1.25	5.84
Motarjemi and Van Horn	1.13	6.37	1.18	6.20
STRUDL with Vehicle in Lanes 1 and 3	1.04	7.04	1.04	7.04
STRUDL with Vehicle in Lanes 1 and 2	1.34	5.46	1.34	5.46
HS-40 Southbound in Lanes 1 and 3	0.96	7.64	1.06	6.91
HS-40 Southbound in Lanes 1 and 2	1.04	7.05	1.44	5.15
HS-40 Northbound in Lanes 1 and 3	1.00	7.33	0.96	7.64
HS-40 Northbound in Lanes 1 and 2	1.14	6.43	1.42	5.64
HS-20 Southbound in Lanes 1 and 3	1.12	6.55	0.82	8.95
HS-20 Southbound in Lanes 1 and 2	1.30	5.31	1.28	6.43

CHAPTER VI

DISCUSSION

Analytical or empirical distribution factors used to assign loads to a particular bridge girder should be large enough to predict the maximum portion of load the girder will experience in service. However, if the distribution factors are too large, more load than necessary will be used in design, resulting in inefficient use of material.

Table 8 (p. 61) and Table 9 (p. 65) compare distribution factors computed by three different empirical methods and one analytical method to distribution factors computed from full scale rolling load test data.

Rolling Load Tests

The maximum (design) distribution factors computed from the test data for Bridge No. 1 are given as:

Interior Girder - 1.38

Exterior Girder - 1.40

The maximum (design) distribution factors computed from the test data for Bridge No. 4 are given as:

Interior Girder - 1.30

Exterior Girder - 1.44

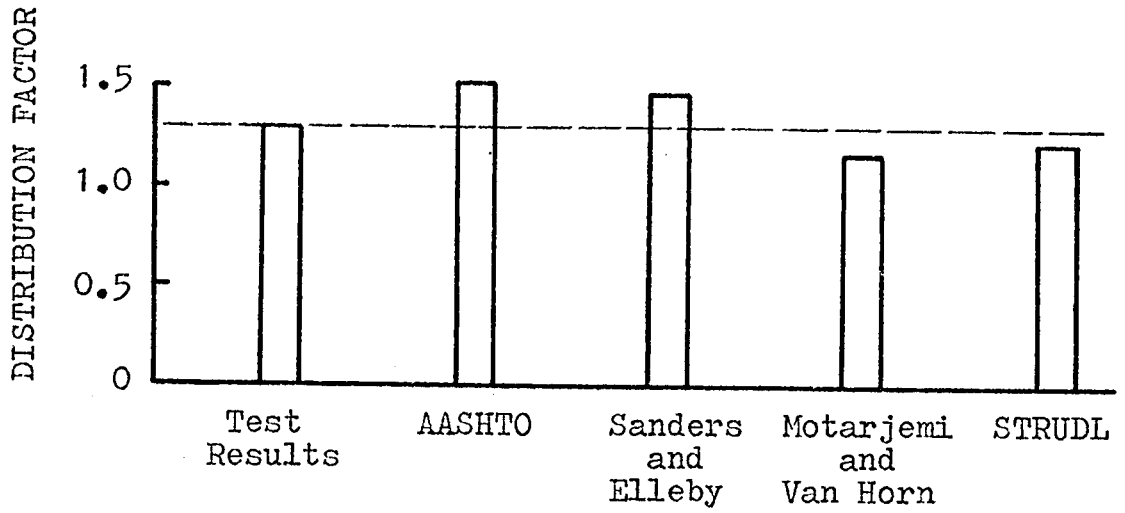
Discussion of Actual and Theoretical Distribution Factors

The accuracy of any empirical or analytical method used to compute lateral distribution of wheel loads is

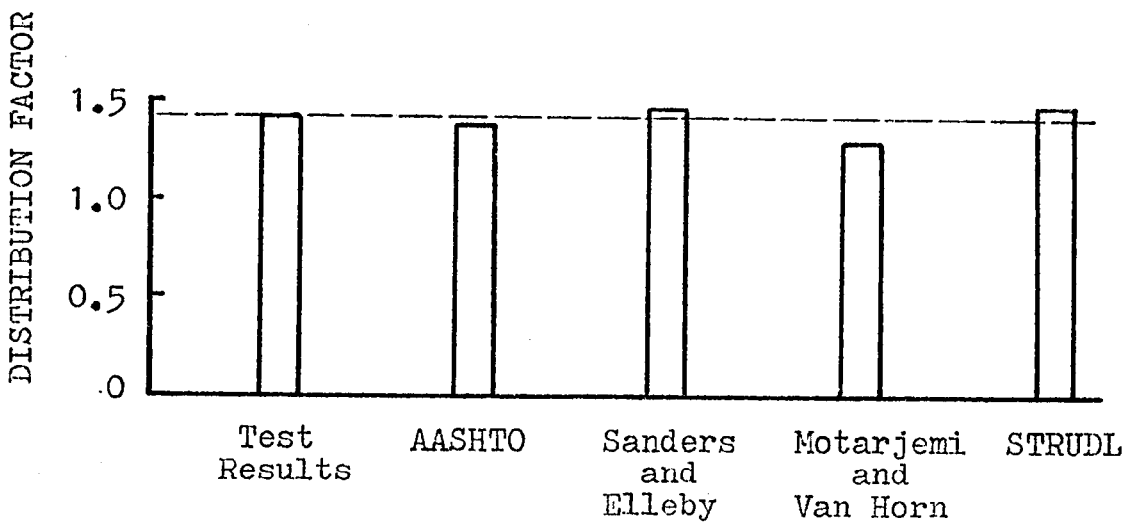
entirely dependent on the assumptions made and the inclusion or exclusion of particular variables. Maximum distribution factors computed from the test data are graphically compared to those computed from the four theoretical methods in Figures 31 and 32.

Test Results. A comparison of values from Tables 8 and 9 shows that the maximum distribution factors for interior girders for the two bridges are different by 6.1% and the maximum distribution factors for exterior girders for the two bridges are different by only 1.4%. According to each of the empirical methods of obtaining lateral distribution, the distribution factors for the interior girders of Bridge 4 should have been significantly smaller than those for Bridge 1 because of the different girder spacings. However, factors such as the composite design of Bridge 1 vs. the non-composite design of Bridge 4; the different girder stiffness to span ratios for the two bridges; and the same stiffness of interior girders in Bridge 1 vs. the extra stiffness of the interior girders in Bridge 4 probably all contributed to offset the small difference in girder spacing.

AASHTO Specifications. The current specifications list several different values of "D" used to determine distribution factors depending on the type of bridge construction. The value 5.5 is used for the interior girders of a concrete deck over steel I-beams - composite or non-composite. Therefore, when the girder spacing is

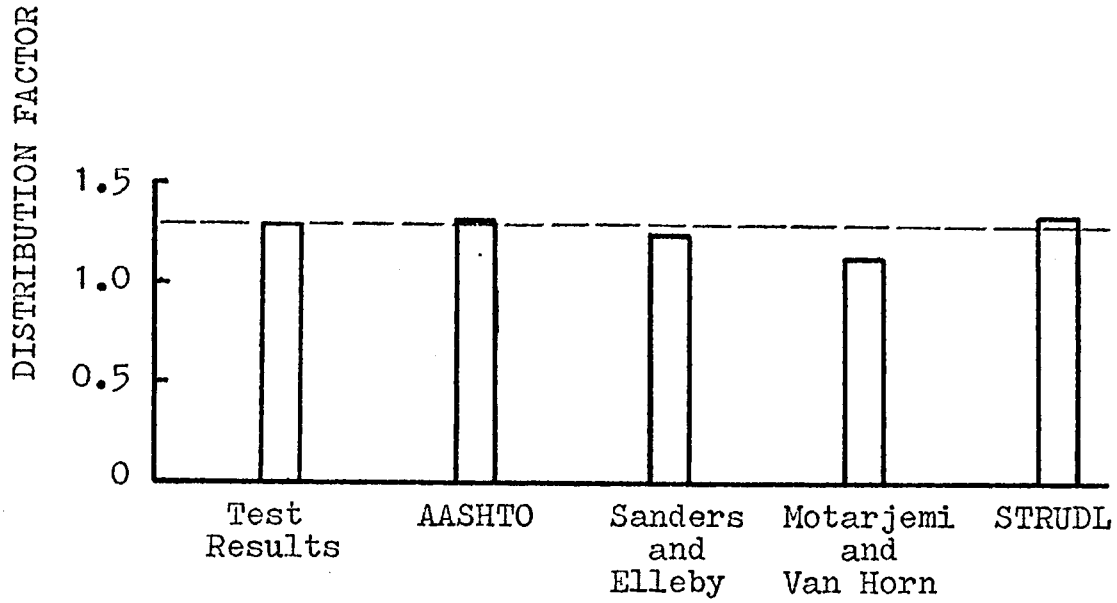


(a) INTERIOR GIRDER

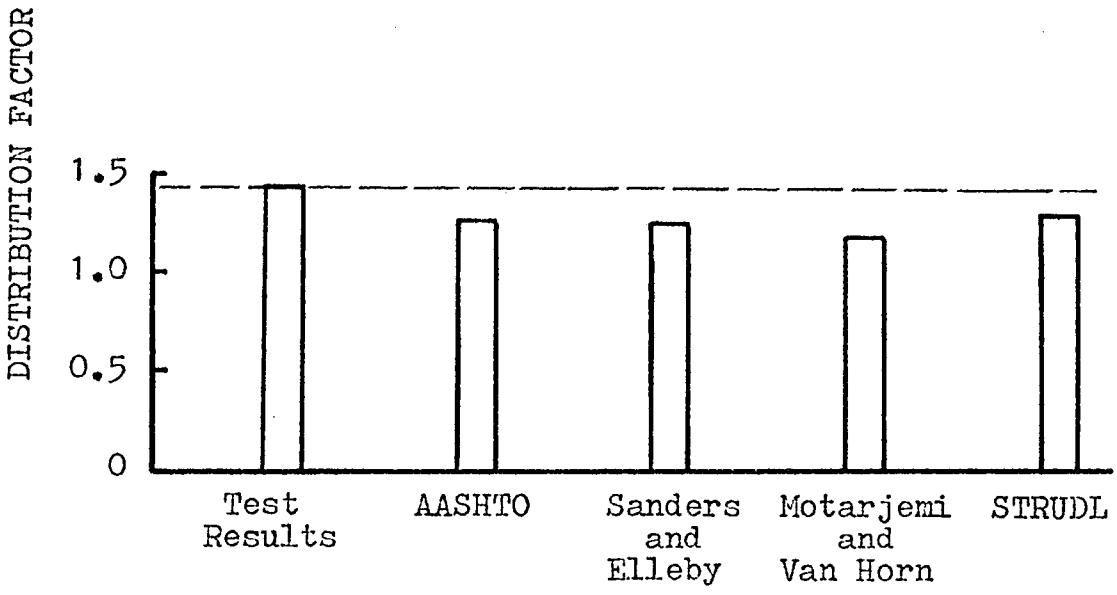


(b) EXTERIOR GIRDER

FIGURE 31. COMPARISON OF ACTUAL AND THEORETICAL DISTRIBUTION FACTORS FOR BRIDGE 1



(a) INTERIOR GIRDER



(b) EXTERIOR GIRDER

FIGURE 32. COMPARISON OF ACTUAL AND THEORETICAL DISTRIBUTION FACTORS FOR BRIDGE 4

reduced, the distribution factor is reduced by the same percentage. The AASHTO interior girder distribution factor is 9.4% above the experimental value for Bridge 2 and 2.5% above the experimental value for Bridge 4. This comparison shows the AASHO factor to be much more closely related to the actual values for a non-composite design than for a composite one. Bogaty observed this same phenomenon in his analysis of Bridge 1 as a composite and non-composite cross section (3). A distribution factor of S/6.0 more closely reflects the maximum load carried by the interior girders of Bridge 1.

The AASHTO exterior girder distribution factor is 2.9% below the experimental value for Bridge 1 and 11.3% below the experimental value for Bridge 4. In this comparison both design values are lower than the actual values. The complete participation of the curbs and partial participation of the guard rails increased the stiffness and thus the distribution factor for the exterior girders in the tests. This addition in load was more than offset by the increase in section modulus, resulting in lower stresses than anticipated. The composite action of the curbs should be considered in the analysis and design of the exterior girders, and their full participation should be assured through proper details.

Sanders and Elleby Proposal. The computed distribution factors are 5.1% and 1.2% above the actual distribution factors for interior and exterior girders, respectively,

of Bridge 1. The computed distribution factors are 3.9% and 12.0% below the actual values for interior and exterior girders respectively of Bridge 4. For the case of fully composite beams such as Bridge 1, the Sanders and Elleby proposal seems to more accurately reflect the true behavior of the interior girders than do the current AASHTO specifications. Since the AASHTO specifications were developed using bridges similar to Bridge 4 they are slightly more accurate in this instance. Sanders and Elleby state that their proposal will effect the most change when the designer optimizes the aspect ratio (width/length) to obtain the most uniform distribution, and a further savings may be obtained by considering the effects of increased girder torsional rigidity and slab thickness. Their proposal differs only slightly from the current specifications for interior girders of bridges of "normal" cross section, width and span.

Sanders and Elleby found that the exterior or the interior beam can be the critical one depending on the bridge properties and loading. The use of the same distribution factor for all girders is valid for their analysis only because they did not include the effect of curbs and handrails, the importance of which has been previously discussed.

Motarjemi and Van Horn. All of the distribution factors calculated using the Motarjemi and Van Horn recommended equations are considerably lower than the test

values and the other empirical values. This is to be expected since their distribution equation was derived from a theoretical analysis of concrete box-beam bridges and then compared to actual test values for the same. Concrete box beam bridges have much better load distribution characteristics than steel girder bridges because of the very high torsional stiffness of the beams. This high torsional stiffness has much the same effect on distribution as a thickened top slab on a steel girder bridge. The AASHTO specifications require a distribution factor of S/7.0 for box beams which is 21.5% lower than the distribution factor of S/5.5 required for steel girders. In their conclusion, Motarjemi and Van Horn state the method of analysis is "a general method applicable to any beam-slab superstructure." They suggest methods to modify their equations and computer program for other bridges. A theoretical analysis of this magnitude is beyond the scope of this thesis but would provide important data for future study.

STRUDL II Analyses. Bridge 1 maximum distribution factors from the STRUDL II analysis are 13.0% below and 11.4% above the experimental distribution factors for interior and exterior girders respectively. The STRUDL II load distribution coefficients tabulated in Reference 3 for exterior girders are consistently 10% to 20% higher than the test values indicating the STRUDL model had a disproportionately stiff exterior girder-curb section. Bogaty also analyzed

Bridge 1 with no composite action between the slab and girders. This analysis yielded results which were slightly closer in magnitude to the actual values but did not appear to reflect the true behavior because the exterior girder distribution factors were less than the interior girder factors.

Bridge 4 maximum distribution factors from the STRUDL II analysis are 3.1% above and 7.46% below the experimental distribution factors for interior and exterior girders respectively. The STRUDL II load distribution coefficients listed by Rush (4) for exterior girders are 5% to 14% below test values. In this case the exterior girder-curb section used in the analysis was also stiffer than that in the actual bridge.

In general each of the theoretical analyses predicted actual bridge behavior quite closely. If care is taken to insure that the relative stiffnesses of the model girders are the same as the actual bridge girders this method can be a very powerful tool in predicting not only load distribution but deflections, moments, and even ultimate capacity as well.

Static Load Tests to Failure

The load distribution coefficients for Bridge 1 are shown in Table 6 (p. 45), and those for Bridge 4 are shown in Table 7 (p. 47). These results illustrate one central fact. The lateral distribution of load is independent of the magnitude of the load. This behavior is exhibited by

both bridges including Bridge 4 under pattern loading. Distribution factors are not computed for the static load tests since the simulated vehicles were placed in their respective design lanes and could not be moved across the bridge.

CHAPTER VII

CONCLUSIONS

The availability of two full size highway bridges designed according to specifications current for the time offered a rare opportunity to experimentally verify design assumptions and various methods of analysis.

The following conclusions relating to the lateral distributions of load are made based on these tests:

(1) The rolling load data suggest that, for a particular bridge, the lateral distribution of load depends almost entirely on the lateral position of the vehicle on the bridge. While axle spacing, magnitude of vehicle load, and vehicle speed have a measurable effect on the total moment at a bridge cross section, these parameters appear to have only a minor effect on the lateral distribution of load to supporting girders.

(2) The static load test data indicate that, as load on a bridge is increased up to the order of magnitude which produces first yield of the steel, the load distribution coefficients are not significantly affected.

(3) The AASHTO specifications require distribution factors which are slightly conservative for interior girders and slightly unconservative for exterior girders, indicating that they do not fully account for the additional stiffness contributed to the exterior girder by curbs and handrails.

(4) The Sanders and Elleby equation yields distribution factors which are conservative for the composite bridge and unconservative for the non-composite bridge. If the non-composite equation is adjusted to account for partial slab participation the factors are in closer agreement. Their exclusion of the effects of curbs and handrails is shown to be invalid.

(5) The Motarjemi and Van Horn recommendations are based on concrete box beam bridges. Due to the high torsional stiffness of box beams, distribution factors computed using their equations are predictably lower than those for steel girder bridges. Their theoretical analysis should be modified and used to check the results reported herein.

(6) The STRUDL II models did not predict distribution factors which were entirely consistent with the experimental values. The relative stiffness of the interior girder-slab section and the exterior girder-slab-curb section appear to have a great deal of effect on the distribution of load. These parameters must be very carefully evaluated and adjusted to insure the model acts like the structure.

(7) While the AASHTO requirements did not predict the actual maximum distribution factors as determined by test results, they were just as accurate, on the average, as all of the other methods reported herein.

(8) The M-60 and HET-70 loads were more evenly distributed due to their wide track or wheel spacings.

LIST OF REFERENCES

LIST OF REFERENCES

1. Varney, Robert F. "Preliminary Research Report of a Highway Bridge Loading Study with the HET-70 Main Battle Tank Transporter," Bureau of Public Roads, Washington, D.C., 1969.

2. Burdette, Edwin G. and David W. Goodpasture. "Final Report on Full Scale Bridge Testing An Evaluation of Bridge Design Criteria," University of Tennessee, Department of Civil Engineering Research Series, 1971.

3. Bogaty, Anton C., Jr. "A Study Concerning Data Input Into a Finite Element Analysis of a Highway Bridge," Unpublished M.S. project paper, The University of Tennessee, Knoxville, 1973.

4. Rush, Albert W., Jr. "A Study of Wheel Load Distribution in a Highway Bridge," Unpublished M.S. project paper, The University of Tennessee, Knoxville, 1973.

5. The American Association of State Highway Officials. "Specifications for Highway Bridges," Washington, D.C., 1973.

6. Sanders, W.W., Jr. and H.A. Elleby. "Distribution of Wheel Loads on Highway Bridges," Iowa State University Engineering Research Institute, Ames, 1968.

7. Motarjemi, Daryoush and David A. Van Horn. "Theoretical Analysis of Load Distribution in Prestressed Concrete Box-Beam Bridges," Fritz Engineering Laboratory Report No. 315.9, Bethlehem, 1969.

8. Douglas W.J. and D.A. Van Horn. "Lateral Distribution of Static Loads in a Prestressed Concrete Box-Beam Bridge," Fritz Engineering Laboratory Report No. 315.1, Bethlehem, 1966.

9. Guilford, A.A. and David A. Van Horn. "Lateral Distribution of Dynamic Loads in a Prestressed Concrete Box-Beam Bridge - Drehersville Bridge," Fritz Engineering Laboratory Report No. 315.2, Bethlehem, 1967.

10. Schaffer, Thomas and David A. Van Horn. "Structural Response of a 45° Skew Prestressed Concrete Box-Girder Highway Bridge Subjected to Vehicular Loading - Brookville Bridge," Fritz Engineering Laboratory Report No. 315.5, Bethlehem, 1967.

11. Guilford, A.A. and David A. Van Horn. "Lateral Distribution of Vehicular Loads in a Prestressed Concrete Box-Beam Bridge - Berwick Bridge," Fritz Engineering Laboratory Report No. 315.4, Bethlehem, 1967.

12. Lin, Cheng-shung and David A. Van Horn. "The Effect of Midspan Diaphragms on Load Distribution in a Prestressed Concrete Box-Beam Bridge - Philadelphia Bridge," Fritz Engineering Laboratory Report No. 315.6, Bethlehem, 1968.

13. Guilford, A.A. and David A. Van Horn. "Lateral Distribution of Vehicular Loads in a Prestressed Concrete Box-Beam Bridge - White Haven Bridge," Fritz Engineering Laboratory Report No. 315.7, Bethlehem, 1968.

14. Van Horn, David A. "Structural Behavior Characteristics of Prestressed Concrete Box-Beam Bridges," Fritz Engineering Laboratory Report No. 315.8, Bethlehem, 1969.

VITA

Edwin A. McDougle, Jr. was born in Chattanooga, Tennessee on November 20, 1946. He attended elementary schools in Knoxville, Tennessee and was graduated from Young High School in 1964. The following September he entered The University of Tennessee at Knoxville, and in June 1969, he received a Bachelor of Science degree in Civil Engineering.

He entered the Graduate School at the University of Tennessee in September 1969 while teaching as an Instructor in the Department of Basic Engineering and Graphics. After serving as a pilot in the Tennessee Air National Guard he returned to Graduate School and received his Master of Science in Civil Engineering in December 1975.

He is currently employed as a structural design engineer by Ross H. Bryan Inc., Consulting Engineers. He is a member of the American Society of Civil Engineers, Tau Beta Pi, Chi Epsilon, and Phi Kappa Phi.

He is married to the former Carla Ann Kastory of Knoxville, Tennessee. They have two children, Allison and Meredith.